ACCSCIENCE PUBLISHING

International Journal of Bioprinting

RESEARCH ARTICLE

Advances in nanomaterial-enhanced bioinks for bone tissue bioprinting

Yuqiang Wang†, Wentao Hu†, Jinbo Zhang, Dedong Liu*, and Zhuoxuan Li*

Department of Orthopedics, The Second Hospital of Jilin University, Changchun, Jilin, China

Abstract

Three-dimensional bioprinting provides a promising strategy for constructing living bone substitutes with controlled architecture, cellular organisation, and regenerative function. However, conventional hydrogel bioinks often struggle to simultaneously achieve sufficient printability, structural stability, and biological activity for bone tissue formation. The incorporation of nanomaterials has therefore emerged as an effective approach to transform hydrogel bioinks into multifunctional composite systems capable of regulating both material properties and the cellular microenvironment. This review first outlines the dynamic process of bone repair, including inflammation, tissue formation, vascularisation, and remodelling, and discusses the requirements that these biological processes impose on bioink design. Major bioprinting technologies, including extrusion-based, inkjet, light-based, coaxial, and embedded bioprinting, are then summarised with particular attention to their compatibility with nanomaterial-containing bioinks. The review subsequently focuses on ceramic nanomaterials, silicates and nanoclays, carbon-based nanomaterials, two-dimensional nanomaterials, and polymeric or fibrous nanomaterials. Their roles in regulating rheological behaviour, print fidelity, mechanical stability, mineralisation, osteogenic differentiation, angiogenesis, and immunomodulation are critically discussed. Current evidence demonstrates that nanomaterial performance is strongly dependent on particle composition, concentration, size, morphology, surface chemistry, dispersion state, and interactions with the surrounding polymer network. Increasing nanomaterial content does not necessarily improve regenerative outcomes and may instead compromise extrusion, photocrosslinking, cellular activity, or long-term structural stability. Future development should therefore move beyond empirical nanoparticle incorporation towards coordinated optimisation of nanomaterial properties, bioink formulation, printing parameters, cellular composition, and degradation behaviour. Such an integrated design framework may enable the development of next-generation bioinks capable of more closely recapitulating the dynamic and multicellular microenvironment required for functional bone regeneration.

Keywords: 3D bioprinting; Bioinks; Nanomaterials; Bone tissue engineering; Bone regeneration; Osteogenesis; Nanocomposite hydrogels

1. Introduction

Large-scale bone defects can arise from severe trauma, infection, tumour resection, and congenital abnormalities. When the extent of tissue loss exceeds the intrinsic

†*These authors contributed equally to this work.*

***Corresponding authors:**
Dedong Liu
(1325103693@qq.com);
Zhuoxuan Li
(lizhuoxuan@jlu.edu.cn)

Citation: Wang Y, Hu W, Zhang J, Liu D, Li Z. Advances in nanomaterial-enhanced bioinks for bone tissue bioprinting. *Int J Bioprint*.
doi: 10.36922/IJB026350383

Received: August 29, 2026

Revised: October 12, 2026

Accepted: October 15, 2026

Published online: November 19, 2026

Copyright: © 2026 Author(s). This is an Open-Access article distributed under the terms of the Creative Commons Attribution License, permitting distribution, and reproduction in any medium, provided the original work is properly cited.

Publisher's Note: AccScience Publishing remains neutral with regard to jurisdictional claims in published maps and institutional affiliations.

regenerative capacity of bone, spontaneous healing is often insufficient to restore complete structural and functional integrity.[1-3] Tissue engineering, through the integration of biomaterials, cells, and bioactive cues, has provided new strategies for developing regenerative bone substitutes. However, conventional scaffold fabrication approaches remain limited in their ability to precisely control internal architecture, spatial cell distribution, and the local microenvironment.[4,5] Three-dimensional (3D) bioprinting enables the spatially controlled deposition of cell-laden bioinks under the guidance of digital models, allowing scaffold architecture, cellular components, and bioactive factors to be organised in a coordinated manner during fabrication and thereby creating new opportunities for the construction of patient-specific, biologically active bone tissues.[6] In recent years, the development of large-scale self-mineralising bone organoids based on cell-laden bioinks, together with immunomodulatory tissue-engineered bone constructs, has further demonstrated that the objective of bioprinting is gradually shifting from simply generating cell-containing scaffolds with predefined geometries towards reconstructing functional microenvironments capable of supporting tissue maturation and bone defect regeneration.[7,8]

Bioinks provide the critical link between bioprinting processes and the regenerative functions of fabricated tissues. Gelatin methacryloyl (GelMA), alginate, hyaluronic acid, and their composite hydrogels provide hydrated and cytocompatible 3D microenvironments and have therefore been widely employed in bone tissue bioprinting. However, hydrogel-only systems often struggle to simultaneously satisfy the requirements of bone tissue engineering for printing fidelity, structural stability, and osteogenic activity.[9] GelMA is a representative example. Its favourable cytocompatibility makes it well suited for cell encapsulation, whereas its relatively limited mechanical stability and intrinsic osteogenic activity constrain its use as a standalone bioink for bone tissue fabrication. Liu *et al.*[10] incorporated nano-attapulgite (ATP) into GelMA and observed improvements in printability and mechanical performance, together with enhanced osteogenic differentiation of bone marrow-derived mesenchymal stem cells (BMSCs) and angiogenic activity of endothelial cells. These effects ultimately translated into improved repair of calvarial defects. A direct comparison of GelMA-based bioinks by Kühl *et al.*[11] further demonstrated that different nanomaterials confer distinct functional advantages. Calcium phosphate (CaP) nanomaterials predominantly enhanced osteogenic differentiation and calcium deposition by human mesenchymal stem cells (hMSCs), whereas graphene oxide (GO) produced a more pronounced increase in elastic modulus. These findings indicate that increasing hydrogel concentration or crosslinking density alone cannot replace the rational selection of bioink components based on specific functional requirements.

Natural bone is itself a multiphasic tissue composed of an organic matrix reinforced by nanoscale inorganic minerals, providing a direct biomimetic rationale for the incorporation of nanomaterials into bioinks. Unlike inert fillers in conventional hydrogels, nanomaterials can simultaneously regulate bioink rheology, crosslinking behaviour, mechanical properties, and the cellular microenvironment through their high specific surface area, surface chemical reactivity, and interfacial interactions with polymer networks.[12,13] A broad range of nanomaterials has consequently been investigated for the development of bone bioinks. Chimene *et al.*[14] incorporated nanosilicates into a GelMA/κ-carrageenan system to develop the nanosilicate-reinforced kappa-carrageenan/GelMA bioink, commonly referred to as the nanoengineered ionic-covalent entanglement (NICE) bioink, which exhibited shear-thinning behaviour and osteoinductive properties. Liu *et al.*[15] subsequently combined nanosilicates with cell-laden hydrogels and showed that these nanomaterials not only improved printability and material performance but also promoted BMSC osteogenesis and enhanced new bone formation in a rat calvarial defect model. Tavares *et al.*[13] developed a GelMA nanocomposite bioink containing mesoporous silica nanoparticles loaded with calcium, phosphate, and dexamethasone. Human BMSCs encapsulated within this system exhibited osteogenic differentiation and matrix mineralisation even in the absence of additional mechanical stimulation. Beyond mineral-based inorganic nanomaterials, GO has been shown to simultaneously modulate shear-thinning behaviour, structural fidelity, and osteogenic differentiation, with these effects displaying a clear concentration dependence.[16] MXenes have also been incorporated into cell-laden GelMA/methacrylated hyaluronic acid (HAMA) systems and shown to support hMSC viability and spontaneous osteogenic differentiation.[17] In addition, nanocellulose can serve as a rheological and structural reinforcing network and can be further combined with hydroxyapatite (HA) or GO. Emerging nanoceramics, such as magnesium (Mg)-doped nano-hydroxyapatite (nHA), are also being explored to optimise bioink printability and cellular responses through deliberate control over particle composition, crystallinity, and morphology.[18,19]

The role of nanomaterials in bone bioinks has progressively expanded beyond simple mechanical reinforcement to encompass the regulation of printing

performance, reconstruction of bone-like mineral microenvironments, and the introduction of osteogenic, angiogenic, and other regenerative functions. However, different nanomaterials operate through distinct mechanisms and provide different dominant functionalities, while their overall effects are further governed by particle size, morphology, concentration, dispersion state, and interactions with the surrounding hydrogel network.[20] Variations in GO concentration, for example, can produce different optimal ranges for printability, mechanical performance, and osteogenic differentiation of hMSCs, whereas CaP and GO incorporated into the same GelMA-based printing system exhibit distinct mechanical and biological advantages.[11] Therefore, the development of nanomaterial-enhanced bioinks should not be simply regarded as the incorporation of nanoscale fillers into conventional hydrogel systems. Instead, it represents an integrated materials engineering strategy that requires a delicate balance among printability, cytocompatibility, and regenerative functionality.[21] It is important to note that current studies on nanomaterial-assisted bone tissue bioprinting encompass diverse experimental paradigms, including the direct incorporation of nanomaterials into cell-laden bioinks for bioprinting, the fabrication of nanocomposite scaffolds followed by subsequent cell seeding, and the investigation of biological mechanisms using non-bioprinted nanomaterial systems.[22,23] Accordingly, this review primarily focuses on the application of nanomaterial-enhanced cell-laden bioinks in bone tissue bioprinting. Studies involving the latter two categories are discussed as complementary evidence to elucidate the intrinsic bioactivities of nanomaterials, their material reinforcement mechanisms, and their implications for the rational design of future bioink systems. Based on this framework, this review first provides an overview of the dynamic progression of bone healing, including the inflammatory, reparative, and remodelling phases. Subsequently, advances in extrusion-based, inkjet-based, light-assisted, coaxial, and embedded bioprinting technologies are introduced. Particular emphasis is placed on recent developments in ceramic nanomaterial-, silicate/nanoclay-, carbon-based nanomaterial-, two-dimensional (2D) nanomaterial-, and polymeric/fibrous nanomaterial-enhanced bioinks for bone tissue bioprinting. By integrating these emerging advances, this review aims to elucidate the interrelationships among nanomaterial composition, bioink properties, cellular responses, and bone regenerative outcomes, thereby providing a conceptual framework for the rational design of next-generation functional bioinks for bone tissue bioprinting (Figure 1).

2. Bone healing process

Bone healing is a dynamic and highly coordinated process involving immune responses, progenitor-cell recruitment and differentiation, angiogenesis, extracellular matrix formation, and tissue remodeling.[24,25] Its progression is influenced by multiple factors, including defect size, anatomical location, local vascular supply, mechanical

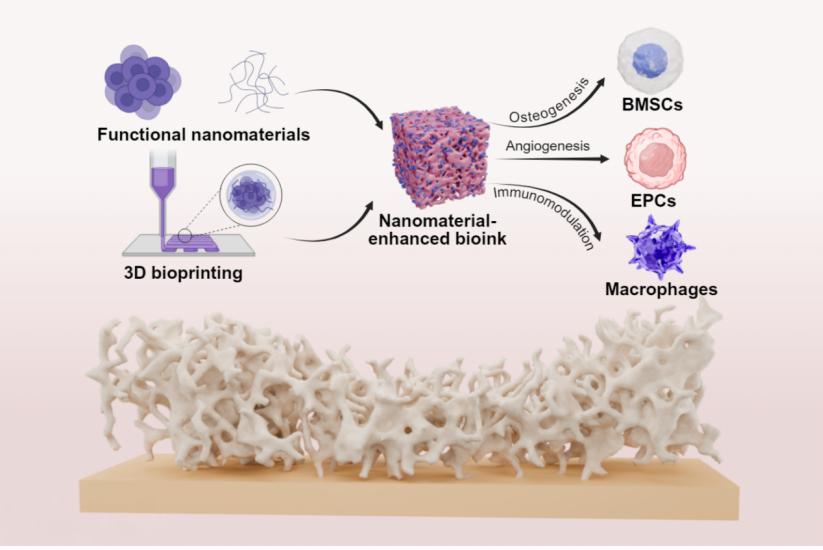


Figure 1. Nanomaterial-enhanced bioinks for bone tissue bioprinting. Functional nanomaterials integrated into hydrogel-based bioinks improve the capacity of 3D-bioprinted constructs to regulate key cellular components of the bone regenerative microenvironment. Their interactions with bone marrow mesenchymal stem cells (BMSCs), endothelial progenitor cells (EPCs), and macrophages contribute to enhanced osteogenesis, angiogenesis, and immunomodulation, collectively facilitating bone regeneration. Created in BioRender.Zhuoxuan Li. (2026) https://BioRender.com/1uq500u. Figure created by the authors.

stability, and host-related conditions. The phases of bone healing are not discrete events but overlap substantially and transition gradually from one to another. In general, bone healing can be broadly divided into the inflammatory phase, the proliferative and reparative phase, and the remodelling phase.[26] The early inflammatory response removes damaged tissue and establishes a regenerative microenvironment. This is followed by progenitor-cell proliferation, neovascularisation, osteogenesis, and chondrogenesis, which collectively drive the formation of new tissue. Subsequently, sustained coupling between bone resorption and bone formation gradually converts the initially formed immature bone into mature tissue with a more organised architecture and improved mechanical competence. Bone healing should therefore not be regarded simply as an osteogenic process, but rather as a temporally evolving regenerative cascade governed by coordinated changes in the immune, vascular, cellular, and mechanical microenvironments.[27] For bone tissue bioprinting, cell-laden constructs implanted into osseous defects are exposed to the same dynamically changing regenerative milieu. Accordingly, their material composition and biological functionality should extend beyond supporting early cell survival and should accommodate the distinct biological requirements associated with inflammatory regulation, vascularisation, osteogenic mineralisation, and subsequent tissue remodelling[28] (Figure 2).

2.1. Inflammatory phase

Following bone injury, disruption of the local vasculature rapidly leads to haematoma formation, while damaged cells and extracellular matrix components release damage-associated molecular patterns that activate the complement system and multiple inflammatory signalling pathways, thereby initiating the early immune response to bone injury.[29] Neutrophils are among the first circulating immune cells recruited to the injured site. They contribute to tissue clearance by phagocytosing cellular debris and releasing reactive oxygen species and proteolytic enzymes, while also producing a range of chemokines and cytokines that regulate the subsequent recruitment of other immune-cell populations.[30] This is followed by extensive infiltration of monocytes, which differentiate into macrophages within the injury site. In addition to removing necrotic tissue, macrophages regulate the recruitment and activation of skeletal stem/progenitor cells and vascular-associated cells through the secretion of inflammatory mediators, chemokines, and growth-related signals.[27] Early inflammation should therefore not be regarded merely as a detrimental response that needs to be suppressed, but

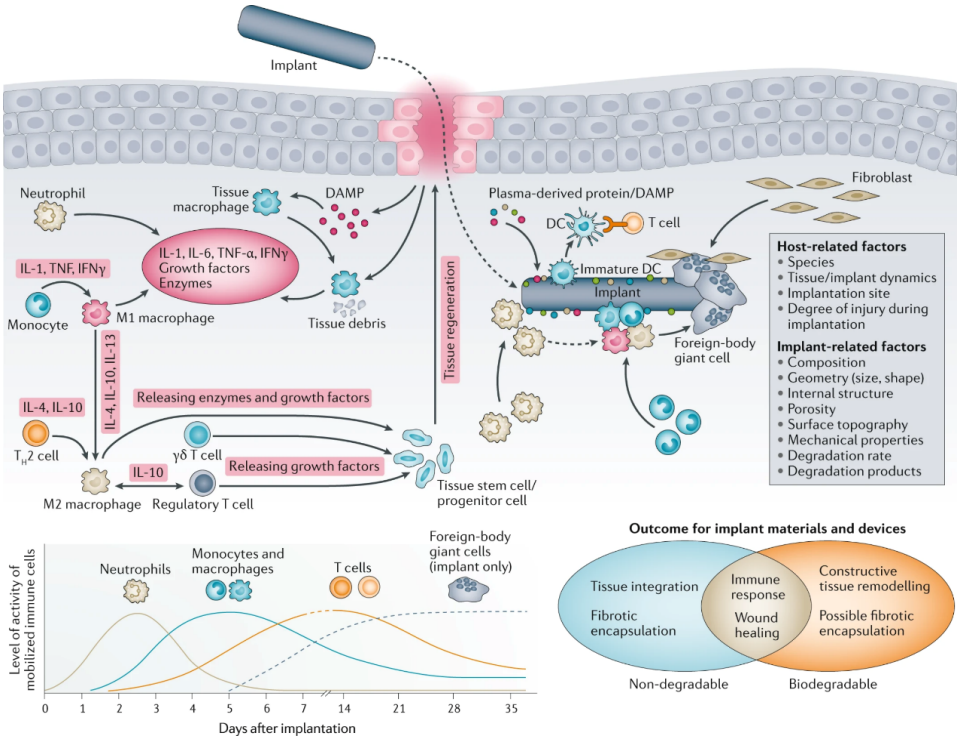


Figure 2. Implant-mediated immune responses interact with the physiological tissue-healing process to determine implant outcomes. The host response to an implanted biomaterial is dynamically integrated with the normal phases of tissue healing, and the balance between inflammatory and regenerative processes ultimately influences tissue integration and repair. Figure reprinted with permission from Li *et al.*[28] Copyright © 2019 Springer Nature Limited. Abbreviations: DAMP: Damage-associated molecular pattern; DC: Dendritic cell; IFNγ: Interferon-gamma; IL: Interleukin; TNF: Tumour necrosis factor.

rather as an essential biological process required for the initiation of bone regeneration.

Recent multimodal analyses of immune-cell populations during bone healing have further revealed pronounced spatiotemporal changes in distinct macrophage subsets within the repair microenvironment, highlighting their role as a critical interface between injury recognition and subsequent bone regeneration. Nevertheless, both the magnitude and duration of inflammation strongly influence the progression of later repair. A transient and appropriately controlled inflammatory response facilitates necrotic tissue clearance and the initiation of regenerative signalling, whereas persistent or excessive inflammation can impair skeletal progenitor-cell function and delay new bone formation. Resolution of inflammation is therefore not simply a passive reduction in pro-inflammatory mediators, but an active process driven by functional transitions in macrophages, clearance of apoptotic cells, and the release of pro-resolving and pro-regenerative signals.[31] Zou *et al.*[32] further demonstrated that macrophages accumulating in aged fracture calluses secrete elevated levels of grancalcin, which induces senescence in skeletal stem/progenitor cells and delays fracture healing, providing direct evidence that a dysregulated immune microenvironment can compromise subsequent bone regeneration. Effective bone healing therefore depends not on non-specific suppression of inflammation, but on maintaining an appropriate early inflammatory response followed by its timely transition towards a regenerative microenvironment. This principle is particularly relevant to nanomaterial-enhanced bioinks, as nanomaterial surface chemistry, particle composition, degradation products, and ion release can all directly influence the early immune response at the implantation site.

The early inflammatory response following bone injury not only determines the efficiency of debris clearance at the damaged site but also represents a critical regulatory window for subsequent angiogenesis and osteogenic initiation.[33] Therefore, nanomaterial-enhanced bioinks have increasingly been recognised as an active strategy for modulating the inflammatory microenvironment rather than merely serving as cell delivery vehicles or structural support materials.[34] By incorporating nanoscale components with immunoregulatory, antioxidant, and ion-releasing properties, bioinks can regulate macrophage polarisation, alleviate excessive inflammatory responses, and facilitate the transition from the inflammatory phase to the regenerative phase during the early stage after implantation. For example, Xu *et al.*[35] developed a 3D-printed strontium (Sr)-containing mesoporous bioactive glass nanoparticle (MBGN)/GelMA nanocomposite scaffold, with cells seeded onto the construct after printing rather than directly encapsulated during fabrication. The sustained release of Sr, calcium (Ca), and silicon (Si) ions contributed to immunomodulation, angiogenesis, and osteogenesis in a diabetic bone defect model. Although the study did not involve direct cell-laden bioprinting, it provides complementary evidence for the potential application of Sr-MBGNs in immunomodulatory bone bioinks.

Similarly, cerium oxide (CeO_2) nanoparticles, owing to their reactive oxygen species-scavenging capacity, can mitigate early oxidative stress after bone injury and further promote osteoblast proliferation and differentiation. Collectively, the role of nanomaterials in bioinks has progressively expanded from conventional mechanical reinforcement towards active immunomodulation. By constructing an immunoregulatory local microenvironment, nanomaterial-enhanced bioinks provide favourable conditions for subsequent tissue repair and regeneration.

2.2. Proliferative phase

As the early inflammatory response gradually resolves, the bone defect enters a reparative stage characterised by cell proliferation, tissue formation, and extracellular matrix deposition. The initial haematoma is progressively replaced by highly cellular and vascularised granulation tissue, while skeletal stem/progenitor cells residing in the periosteum, bone marrow, and surrounding tissues become activated and migrate towards the injury site. Under the influence of local biochemical and mechanical cues, these progenitor populations subsequently undergo osteogenic or chondrogenic differentiation.[36] Importantly, progenitor cells from different anatomical sources do not contribute equally to all forms of bone injury. Jeffery *et al.*[37] demonstrated that skeletal stem/progenitor cells derived from the bone marrow and periosteum fulfil distinct regenerative roles. Bone marrow-derived cells predominantly contributed to the repair of localised bone injuries, whereas periosteal cells represented a major source of newly formed tissue following more extensive injuries, such as bicortical fractures. Liu *et al.*[38] subsequently showed that progenitor cells located within the fibrous layer of the periosteum are rapidly activated after fracture and continue to contribute to the formation and long-term maintenance of newly formed bone. In addition, Julien *et al.*[39] demonstrated that mesenchymal progenitor cells originating from adjacent skeletal muscle can directly contribute to cartilage and bone formation within the callus under specific injury conditions, indicating that the cellular sources supporting bone regeneration are not confined to bone tissue itself. New bone formation during

this stage proceeds primarily through intramembranous and endochondral ossification. In regions with adequate vascular supply and a relatively stable mechanical environment, skeletal progenitor cells can differentiate directly into osteoblasts, which subsequently deposit an osteoid matrix rich in type I collagen that progressively mineralises to form woven bone. In contrast, in regions characterised by local hypoxia or a distinct mechanical environment, progenitor cells may first undergo chondrogenic differentiation and generate a cartilaginous intermediate. Chondrocytes then become hypertrophic, the extracellular matrix undergoes mineralisation and progressive resorption, and the cartilage template is ultimately replaced by newly formed bone. These two modes of ossification are not mutually exclusive and can coexist within the same repair site in different spatial proportions. Their relative contributions are determined by factors including vascular status, tissue strain, and local mechanical stability.[40] During endochondral ossification, removal of mineralised cartilage is itself an actively regulated process. Sivaraj *et al.*[40] identified septoclasts derived from mesenchymal stromal cells and demonstrated that these cells re-emerge during fracture repair, where they participate in matrix resorption during the transition from mineralised cartilage to bone tissue.

Angiogenesis proceeds in parallel with tissue formation during this phase. Newly formed blood vessels not only provide oxygen and nutrients to the regenerating tissue but also facilitate the delivery of circulating cells and multiple paracrine signals, making vascularisation a critical prerequisite for the formation of large volumes of new bone. Recent evidence, however, indicates that the relationship between angiogenesis and osteogenesis is more complex than a simple proportional association. Using longitudinal intravital imaging and single-cell analysis of calvarial regeneration, Bixel *et al.*[41] found that alterations in early vascular sprouting induced through modulation of endothelial vascular endothelial growth factor (VEGF) and Notch signalling were not accompanied by proportional changes in the progression of intramembranous ossification. These findings suggest that although vascularisation is essential for sustaining a regenerative tissue environment, its coupling with osteogenesis is strongly influenced by anatomical location, the mode of ossification, and the temporal stage of repair. Accordingly, during the proliferative and reparative phase, bioprinted bone constructs must simultaneously support progenitor-cell survival and migration, extracellular matrix formation, nutrient and metabolite exchange, vascular ingrowth, osteogenic differentiation, and matrix mineralisation.

During the bone regeneration process, the formation of new blood vessels is highly coupled with the recruitment, proliferation, and osteogenic differentiation of mesenchymal stem cells (MSCs).[42] However, conventional hydrogel-based bioinks often exhibit insufficient mechanical stability and limited long-term bioactivity, making it challenging to simultaneously meet the requirements for cell survival, structural fidelity, and functional induction.[43] The incorporation of nanomaterials provides a promising solution to overcome these limitations. On the one hand, nanoparticles can improve the printing accuracy and structural stability of bioinks by enhancing network crosslinking and optimising rheological properties; on the other hand, their surface bioactivity and ion-releasing capabilities can further regulate cellular behaviours.[44] For instance, dynamic composite bioinks reinforced with copper (Cu)-doped MBGNs exhibit enhanced printability and structural stability, while facilitating angiogenesis and osteogenic differentiation of BMSCs through sustained Cu ion release without the need for additional exogenous growth factors.[9] In addition, nanoclay-reinforced bioinks can improve the rheological properties and drug retention capacity of hydrogel systems, while supporting 3D BMSC culture and vascularised bone tissue formation.

2.3. Remodelling phase

The newly formed bone generated during the reparative phase remains structurally and mechanically distinct from mature native bone. Early osseous callus and woven bone exhibit a relatively disorganised architecture and therefore undergo prolonged remodelling, during which they are progressively replaced by highly organised lamellar bone and the original cortical and trabecular architecture is gradually restored.[45] This process depends primarily on sustained and coordinated interactions among osteoclasts, osteoblast-lineage cells, and osteocytes. Osteoclasts initially resorb mineralised cartilage, immature woven bone, and damaged bone matrix, after which osteoblasts are recruited to the resorption surfaces and deposit new bone matrix. This sequential coordination between bone resorption and bone formation, commonly referred to as remodelling coupling, represents a central mechanism through which bone architecture and mechanical competence are restored.[46,47]

Bone remodelling should therefore not be viewed simply as the passive removal of excessive callus. Increasing evidence indicates that osteoclast-mediated bone resorption also generates biochemical signals that promote subsequent bone formation. Ma *et al.*[46] demonstrated that apoptotic bodies released by osteoclasts can enhance osteoblast differentiation, thereby contributing to the coupling between bone resorption and

formation. Conversely, osteoblast-lineage cells can also regulate the transition of bone tissue from a formative to a resorptive state. Uenaka *et al.*[48] identified a population of extracellular vesicles released by mature osteoblasts that suppress bone formation while promoting osteoclast differentiation, revealing bidirectional intercellular communication between osteogenic and osteoclastic lineages. Through this sustained coupling, the initially formed woven bone is progressively replaced by more highly organised lamellar bone, while bone mass and trabecular architecture are further adjusted in response to the local mechanical environment. Bone remodelling can persist long after structural bridging of the defect has been achieved, indicating that radiographically detectable new bone formation does not necessarily signify complete restoration of functional bone tissue. As physiological loading is progressively re-established, mechanosensory networks within bone continue to regulate the balance between bone formation and resorption, allowing the regenerated region to gradually approach native bone in terms of geometry, mineralisation, and mechanical performance.[48] This prolonged phase also has important implications for the design of bioprinted materials. An ideal bioink should not merely preserve the printed architecture during the early stages of repair, but should also permit progressive replacement of the artificial matrix by newly deposited extracellular matrix. Accordingly, the long-term degradation behaviour, biosafety, and mineralisation characteristics of nanomaterial-enhanced bioinks, together with their interactions with osteoclasts and osteoblasts, should be incorporated into the design and evaluation framework for bone-regenerative materials.

The bone remodelling phase involves the maturation, mineralisation, and structural stabilisation of newly formed bone tissue.[14] Nanomaterials may support these processes through sustained ion release, antioxidant activity, and regulation of cell-material interactions.[49] As complementary scaffold-based evidence, Zhao *et al.*[50] developed digital light processing (DLP)-printed HA bioceramic scaffolds reinforced with cerium-containing mesoporous bioactive glass nanoparticles (BGNs), demonstrating improved mechanical, antioxidant, and osteogenic properties. Similarly, Zhang *et al.*[51] incorporated CeO_2 nanoparticles into 3D-printed bioactive glass scaffolds, which alleviated oxidative stress and enhanced osteogenic responses and bone regeneration. Importantly, both studies employed printed scaffolds rather than cell-laden bioinks and should therefore be considered complementary evidence of nanomaterial bioactivity. These findings nevertheless provide valuable insights into the future design of nanomaterial-enhanced bioinks for supporting bone maturation and remodelling.

3. Bioprinting technologies

Three-dimensional bioprinting provides a manufacturing platform for constructing bone tissue with predefined geometries, cellular distributions, and local microenvironments through digitally controlled spatial organisation of cells, biomaterials, and functional components. Different bioprinting techniques exhibit distinct characteristics in terms of material transport, deposition methods, and solidification mechanisms, thereby imposing different requirements on bioink viscosity, rheological behaviour, crosslinking kinetics, cell density, and particle size.[52,53] According to the current classification framework for bioprinting technologies, this section categorises these techniques into three major groups: extrusion-based bioprinting, jetting-based bioprinting, and vat photopolymerisation-based bioprinting. Specifically, extrusion-based bioprinting encompasses conventional extrusion, coaxial, and embedded bioprinting; jetting-based bioprinting mainly includes inkjet and laser-assisted bioprinting (LAB); and vat photopolymerisation-based bioprinting primarily comprises stereolithography (SLA) and DLP. This classification is particularly relevant to nanomaterial-enhanced bioinks for bone regeneration, as nanoparticles can not only modify the rheological properties, mechanical stability, and biological activity of bioinks but may also induce particle aggregation, jetting instability, light scattering, or reduced crosslinking efficiency. Therefore, the composition of nanomaterials, bioink properties, and specific printing mechanisms should be synergistically designed to achieve an appropriate balance among printing precision, cytocompatibility, structural stability, and bone regenerative functionality.

3.1. Extrusion-based bioprinting

3.1.1. Conventional extrusion bioprinting

Extrusion-based bioprinting utilises pneumatic pressure, piston-driven, or mechanical extrusion systems to continuously dispense cell-laden bioinks through nozzles, enabling the fabrication of filamentous structures according to predefined printing paths. Due to its broad material compatibility, this approach can accommodate relatively high-viscosity hydrogels and high cell-density formulations, while allowing the incorporation of ceramic particles, nanomaterials, and bioactive factors, making it one of the most widely adopted bioprinting technologies for bone tissue engineering. Stable extrusion generally requires bioinks to exhibit pronounced shear-thinning behaviour and appropriate yield stress characteristics, enabling smooth flow through the nozzle while maintaining structural integrity after deposition.[54,55] Oh

et al.[55] developed a machine learning model integrating rheological parameters and printing conditions to predict printing resolution. Their findings suggest that extrusion fidelity depends on multiple interacting factors rather than viscosity alone. Identical bioink formulations may produce substantially different printing outcomes across printing platforms and processing conditions, further emphasising the necessity of jointly optimising extrusion pressure, printing speed, and material rheological properties.[56] For bone tissue fabrication, a balance must be achieved between structural fidelity and the cellular microenvironment. Zhang *et al.*[57] employed extrusion bioprinting of alginate/gelatin-based bioinks containing hMSCs and demonstrated that softer scaffolds with an elastic modulus of approximately 0.66 kPa generated a mineralised tissue volume of 43.5 ± 7.1 mm^3 after 42 days, whereas stiffer scaffolds produced only 22.6 ± 6.0 mm^3. The softer constructs also exhibited higher alkaline phosphatase (ALP) activity and enhanced osteogenic phenotypes. These findings indicate that increasing hydrogel stiffness does not necessarily result in improved bone formation. Moreover, the extrusion process itself imposes mechanical stresses on encapsulated cells. By combining computational fluid dynamics simulations with machine learning analysis, Zhang *et al.*[58] revealed that bioink viscosity, nozzle-induced shear stress, and cell residence time collectively influence post-printing cell viability, indicating that high-viscosity or high-pressure conditions adopted to improve printing precision may simultaneously induce additional cellular damage.

The high compatibility of extrusion-based bioprinting with composite materials makes it particularly suitable for the fabrication of nanomaterial-enhanced bone bioinks. Chimene *et al.*[14] incorporated nanosilicates into a GelMA/κ-carrageenan system to develop a nanocomposite bioink with shear-thinning behaviour and osteoinductive properties. Liu *et al.*[15] further introduced nanosilicates into a gelatin/alginate cell-laden bioink system and demonstrated that the addition of 2% nanosilicates increased the compressive modulus of hydrogels from approximately 47 kPa to 101 kPa, enabled the printing of structures with a height of up to 15 mm, and simultaneously enhanced BMSC osteogenic differentiation and repair of 8 mm critical-sized rat calvarial defects. Zhu *et al.*[9] developed a dynamic nanocomposite bioink reinforced with Cu-doped mesoporous BGNs, which promoted both osteogenesis and angiogenesis while maintaining high cellular viability. Subsequently, the incorporation of calcium silicate nanowires, multicellular systems, and neurovascularised bone bioprinting strategies further demonstrated that extrusion-based printing has evolved beyond simple cell encapsulation towards an advanced manufacturing platform capable of simultaneously regulating structural organisation, cellular interactions, and bioactive component delivery.[59]

The ability to precisely configure materials and cells has further enabled the development of more sophisticated bone regenerative constructs. Shen *et al.*[60] directly printed endothelial cells within interconnected channels of BMSC-laden scaffolds, generating vascular networks that enhanced angiogenic and osteogenic processes and promoted new bone formation in a rat critical-sized calvarial defect model. Sun *et al.*[61] further constructed osteon-like structures containing central medullary cavities, Haversian canals, and Volkmann canals using polycaprolactone frameworks combined with cellular bioinks, achieving enhanced vascularisation and bone formation *in vivo*. The major advantage of extrusion-based bioprinting lies not only in its ability to process high-viscosity bioinks but also in its capacity to spatially organise multiple materials, cell types, and localised biological signals according to predefined architectures.[62] Nevertheless, its limitations remain associated with the trade-off among printing resolution, material viscosity, and cellular viability. In addition, nanoparticle aggregation and nanomaterial-induced alterations in rheological behaviour require careful consideration during the future design of advanced bioink systems.[63]

3.1.2. Coaxial bioprinting

Coaxial bioprinting utilises nozzles equipped with two or more concentric channels to simultaneously deliver different materials, enabling the direct formation of core–shell or hollow fibre structures during deposition. Compared with conventional extrusion-based printing, coaxial bioprinting allows different cell populations, biomaterials, and bioactive factors to be spatially confined within specific regions while simultaneously generating continuous luminal structures, providing distinct advantages for bone tissue constructs requiring coordinated regulation of osteogenesis and angiogenesis.[64,65] By further increasing the number of coaxial channels, tri-axial or multi-axial architectures can be achieved, enabling the spatial organisation of bone-like matrix regions, vascular compartments, and nutrient transport channels within a single printing process.[66]

Ghahri *et al.*[67] developed osteon-like cellular scaffolds using a customised four-layer coaxial nozzle. A sacrificial material was introduced into the innermost layer to generate Haversian canal-like channels, while the adjacent layer encapsulated human umbilical vein endothelial cells (HUVECs) and VEGF-loaded nanoparticles, and the outer layer incorporated hMSCs together with

whitlockite and HA nanoparticles to mimic the mineral microenvironment of lamellar bone. The incorporation of mineral nanoparticles increased the elastic modulus of the nanocomposite hydrogel from approximately 35 kPa to 80 kPa, while maintaining approximately 94% cell viability after 10 days of culture. After two weeks of culture, a significant increase in ALP activity was observed, followed by the formation of abundant mineralised extracellular matrix after three weeks. Zhang *et al.*[68] further developed vascularised tissue-engineered bone constructs through tri-axial bioprinting. In this system, the outer GelMA/alginate layer incorporated nano beta-tricalcium phosphate (β-TCP) and encapsulated MC3T3-E1 cells, the intermediate layer contained HUVECs, and the inner layer utilised gelatin as a sacrificial material to generate continuous nutrient channels. This design enabled the spatial compartmentalisation of osteogenic and vascular regions while preserving internal transport pathways, thereby providing a more favourable nutrient exchange network for the fabrication of thick bone tissue constructs. The major significance of coaxial bioprinting lies not merely in the generation of hollow structures but in its ability to achieve spatial compartmentalisation of multifunctional components. For nanomaterial-enhanced bone bioinks, osteoinductive nanomaterials can be selectively incorporated into the outer bone-like matrix region, whereas pro-angiogenic components can be localised within inner layers or adjacent to vascular channels, thereby minimising potential interference between different functional components. Nevertheless, the simultaneous extrusion of multiple streams increases the complexity of matching material viscosity, flow rates, and crosslinking kinetics. Variations in the flow behaviour of any individual layer may compromise the final lumen dimensions and interfacial stability of the printed constructs.

3.1.3. Embedded bioprinting

Embedded bioprinting involves the deposition of bioinks within a support medium exhibiting yield stress and self-healing capabilities. The supporting bath undergoes localised deformation and flow during nozzle movement and subsequently recovers its structure after nozzle withdrawal, thereby providing temporary mechanical support for the freshly deposited soft materials.[69] This approach reduces the reliance of conventional freeform extrusion on the intrinsic viscosity and rapid solidification capacity of bioinks, making it particularly suitable for collagen-based materials, low-concentration hydrogels, and high cell-density systems. In bone tissue bioprinting, this feature enables soft bioinks with excellent cytocompatibility but insufficient self-supporting ability to maintain complex 3D architectures, while also providing greater flexibility for incorporating inorganic components such as HA and CaP.[70]

Guo *et al.*[71] employed a gelatin-based support bath to print HA/collagen composite constructs containing BMSCs. The support bath maintained the intended geometry of HA/collagen constructs at room temperature and prevented the collapse of low-viscosity collagen after deposition. The incorporation of HA improved the mechanical properties of the composite system, while the printed BMSCs maintained high viability and proliferation capacity accompanied by enhanced ALP expression. The study directly demonstrated that embedded bioprinting can overcome the inherent challenge of collagen-based biomimetic bone materials, which exhibit excellent biocompatibility but limited printing stability.

Embedded bioprinting also enables improved control over cell density and local microenvironmental regulation. Abaci and Guvendiren[72] printed dense hMSC aggregates within HAMA (termed MeHA in the cited study) hydrogels and spatially modulated the composition of the supporting hydrogel to regulate the local extracellular matrix environment, thereby achieving region-specific control of hMSC osteogenic differentiation. Building upon this strategy, Truong *et al.*[73] incorporated human bone allograft particles or tricalcium phosphate particles into HAMA support matrices for embedded printing of high-density hMSC constructs. All groups exhibited cell viability above 95% after printing, while human bone particles significantly enhanced ALP activity and calcium deposition, with concentration-dependent osteogenic responses observed even under basal culture conditions. Importantly, the support bath is not merely a temporary mechanical medium but can also function as a bioactive matrix capable of regulating cellular differentiation. The particle size and rheological properties of the support medium itself also critically influence printing fidelity. Zhang *et al.*[74] developed a cationically crosslinked κ-carrageenan submicron gel support bath and achieved high structural fidelity during the fabrication of complex architectures, including cardiac, tracheal, and branched vascular structures, while maintaining BMSC viability above 92.1% within the printed constructs. Fang *et al.*[75] further developed a reversible template-assisted embedded printing strategy that enabled simultaneous fabrication of complex organ-scale geometries and free-form vascular networks, demonstrating that support media can substantially expand the design space of conventional layer-by-layer printing, particularly for overhanging structures and intricate internal channels.

Compared with conventional freeform extrusion bioprinting, embedded bioprinting offers greater flexibility for processing soft, low-viscosity bioinks; however, the printing outcome is simultaneously governed by the rheological properties of both the bioink and the supporting bath. Excessively rigid support media may increase nozzle resistance and impose greater mechanical stress on encapsulated cells, whereas overly soft media may fail to maintain the deposited architecture. Therefore, for nanomaterial-enhanced bone bioinks, it is necessary to simultaneously evaluate the effects of nanoparticles on bioink flow behaviour and their interfacial interactions with supporting media. Although the number of embedded bioprinting studies specifically targeting bone regeneration remains lower than that of conventional extrusion-based approaches, recent advances indicate substantial potential for this technology in high cell-density fabrication, low-viscosity bone-mimetic matrices, and the construction of spatially heterogeneous regenerative architectures.

3.2. Jetting-based bioprinting

3.2.1. Inkjet bioprinting

Inkjet-based bioprinting utilises thermal actuation, piezoelectric actuation, or other droplet-generation mechanisms to deposit cell- and biomaterial-containing microdroplets at predefined locations. This technology features non-contact deposition, relatively high printing speed, and precise spatial control; however, stable droplet formation requires bioinks to maintain relatively low viscosity and appropriate surface tension, resulting in a narrower range of compatible materials compared with extrusion-based bioprinting.[54] In addition, particle aggregation and cell clustering may compromise nozzle stability, thereby limiting the application of high-solid-content nanocomposite bioinks. Li *et al.*[52] systematically summarised that material rheology, droplet formation dynamics, nozzle dimensions, and crosslinking kinetics are critical factors governing the stability of inkjet bioprinting. In recent years, a major focus in the development of inkjet technology has been expanding the printable viscosity range of hydrogel-based materials. Suntornnond *et al.*[76] modulated the molecular and rheological properties of GelMA through saponification and thermal treatment, enabling stable thermal inkjet printing of 4% modified GelMA while maintaining favourable cell viability and proliferation. Zhu *et al.*[77] further developed a multiphysics-controlled piezoelectric inkjet printing strategy by synchronously regulating printhead pressure and droplet temperature, allowing 5% GelMA to remain printable and undergo rapid gelation after deposition. This approach enabled the fabrication of cell-laden vascular-like structures with an aspect ratio of up to 4.0, without significant impairment of smooth muscle cell viability during printing. These studies demonstrate that precise regulation of droplet formation and gelation processes can partially overcome the conventional limitations of inkjet printing associated with low-viscosity material requirements.

Although direct applications of inkjet bioprinting in bone tissue engineering remain fewer than those of extrusion-based approaches, existing studies have demonstrated its capability for the precise deposition of cells and inorganic nanocomponents. Gao *et al.*[78] co-printed bioactive nanoparticles and hMSCs within 3D hydrogel systems and found that the incorporated nanoparticles enhanced osteogenic differentiation of printed cells and promoted bone-like tissue formation. Subsequently, by synchronously depositing polyethene glycol and GelMA followed by photocrosslinking, printed hMSCs maintained viability above 80% while preserving their osteogenic and chondrogenic differentiation capacities.[79] It should be noted that the printing process itself is not completely biologically inert. Ablanedo Morales *et al.*[80] demonstrated that thermal inkjet printing could induce substantial transcriptional and phenotypic alterations in cells, suggesting that evaluating the cytocompatibility of inkjet printing solely based on short-term post-printing viability may be insufficient.

For nanomaterial-enhanced bone bioinks, inkjet printing is more suitable for nanoscale components with low concentrations, high dispersion stability, and relatively small particle sizes. Excessive nanoparticle loading can increase viscosity and elevate the risk of nozzle clogging; therefore, compared with extrusion-based systems, its application in high-solid-content nanoceramic formulations and highly viscous nanocomposite hydrogels remains limited. Future advantages of inkjet bioprinting in bone tissue engineering may primarily lie in the high-precision spatial deposition of cells, nanoparticles, and bioactive molecules rather than in the continuous fabrication of mechanically robust, high-loading structural constructs.

3.2.2. Laser-assisted bioprinting

Laser-assisted bioprinting is typically based on laser-induced forward transfer (LIFT) for material deposition and can be categorised as a jetting-based bioprinting approach. A typical LAB system consists of a pulsed laser source, a transparent donor substrate, a laser-absorbing layer, a thin bioink film, and a receiving substrate. Upon laser irradiation, the absorption layer generates transient localised energy and vapourisation-induced cavitation bubbles, which drive the formation of microjets and

transfer the bioink onto predefined locations in the form of droplets.[81,82] Unlike inkjet and extrusion-based bioprinting, LAB does not rely on nozzles, thereby avoiding nozzle clogging caused by particles or high-density cell suspensions and reducing continuous nozzle-induced shear stress on encapsulated cells, while enabling more precise control over cell density and spatial distribution. The nozzle-free nature of LAB provides certain advantages for particle-containing bioinks; however, the incorporation of nanomaterials can still directly influence droplet formation dynamics. Bioink viscosity, surface tension, donor layer thickness, laser pulse energy, and the distance between donor and receiving substrates collectively determine jet stability and droplet size. In nanomaterial-enhanced systems, nanoparticle concentration and dispersion state may further alter local energy absorption and fluid dynamic behaviour, while excessive solid loading or particle aggregation can result in unstable jet formation and heterogeneous deposition.[82] Therefore, LAB does not completely eliminate the processing challenges associated with nanocomposite bioinks; rather, it shifts the major processing considerations from nozzle-based flow control towards precise regulation of laser energy, thin-film characteristics, and droplet generation mechanisms.

The study by Keriquel *et al.*[81] provided direct evidence supporting the application of LAB in nanomaterial-enhanced bone tissue bioprinting. In the study, a collagen layer containing 1.2 wt% nHA was first printed into mouse calvarial defects, followed by the spatial deposition of BMSCs with different geometric arrangements, and subsequent printing of an additional nHA-collagen layer on top. Compared with annular cell distribution, the disk-shaped cell arrangement generated greater new bone formation at both 1 and 2 months after implantation, accompanied by significantly increased bone volume/total volume (BV/TV) in the central defect region and the formation of more mature bone tissue at 2 months. These findings demonstrate that the value of LAB extends beyond nozzle-free deposition, as its high spatial resolution enables precise organisation of cells and mineral components, thereby influencing subsequent bone regeneration outcomes. Nevertheless, direct applications of LAB in bone tissue bioprinting remain considerably fewer than those of extrusion-based and DLP-based technologies. Limitations associated with equipment cost, donor ribbon preparation, printing area, and the efficiency of constructing large-scale 3D tissues continue to restrict its broader application.

3.3. Vat photopolymerisation-based bioprinting

3.3.1. Stereolithography

Stereolithography enables the layer-by-layer fabrication of 3D structures through selective photopolymerisation within liquid photosensitive bioresins. Conventional SLA typically employs a focused laser to perform point-by-point scanning along predefined trajectories, inducing localised crosslinking of hydrogels containing polymerisable functional groups. After completion of each layer, the next layer is subsequently constructed to generate the final 3D architecture. Since the fabrication process does not require bioinks to pass through nozzles, SLA can avoid extrusion-induced shear stress while achieving high spatial resolution and smooth surface morphology. GelMA, PEGDA, and other methacrylated natural polymers can serve as photosensitive matrices for SLA-based bioprinting. Wang *et al.*[83] developed a GelMA-based SLA bioprinting system using eosin Y as a visible-light photoinitiator, successfully fabricating cell-laden constructs and demonstrating sustained cellular proliferation and the formation of 3D cellular networks after printing, suggesting that optimising photoinitiation systems may reduce the adverse effects of conventional ultraviolet-induced crosslinking on cell viability.

For nanomaterial-enhanced bone bioinks, the major challenges associated with SLA arise primarily from light propagation and polymerisation kinetics rather than conventional extrusion-related rheological requirements. Nanoparticles such as nHA, CaP, and GO can enhance biomimetic mineralisation, mechanical properties, and biological activity; however, they may also induce light scattering or absorption, thereby altering effective curing depth and interlayer crosslinking efficiency. Therefore, nanoparticle concentration, size, refractive index, and dispersion stability must be optimised in conjunction with photoinitiator concentration, irradiation wavelength, and exposure dosage. Previous studies on SLA-based bone biomaterials have demonstrated that nHA can be effectively incorporated into photopolymerized nanocomposite systems and improve osteogenic responses.[83,84] However, a considerable proportion of these studies employ a strategy involving scaffold fabrication followed by cell seeding rather than true cell-laden bioprinting. Haghpanah *et al.*[84] utilised masked SLA to fabricate printable nHA-containing nanocomposites, demonstrating that increased nHA content improved mechanical properties and enhanced osteoblast adhesion and proliferation. Therefore, compared with DLP-based bioprinting, current evidence supporting the direct application of conventional SLA for nanomaterial-enhanced cell-laden bone bioinks remains relatively limited. Existing efforts have primarily focused on expanding the range of cytocompatible photosensitive materials and minimising light-induced and free radical-associated cellular damage.

3.3.2. Digital light processing

Digital light processing also enables layer-by-layer fabrication through photopolymerisation; however, unlike the point-by-point scanning mechanism of SLA, DLP utilises digital micromirror devices or projection systems to simultaneously project an entire 2D pattern onto each printing layer, allowing a complete cross-section to be cured in a single exposure. Consequently, the printing time of DLP is primarily determined by the number of layers rather than the geometric complexity of individual layers, providing higher fabrication efficiency while maintaining high spatial resolution.[82] This nozzle-free, area-based photopolymerisation strategy is particularly suitable for photocrosslinkable bioinks such as GelMA, methacrylated alginate (AlgMA), and HAMA, enabling the construction of complex porous architectures and spatially organised cellular distributions with minimal mechanical disturbance.

Digital light processing represents one of the most directly supported light-based bioprinting technologies for nanomaterial-enhanced bone bioinks. Kühl *et al.*[11] incorporated CaP nanomaterials and GO separately into GelMA matrices and directly encapsulated hMSCs for DLP bioprinting. The CaP-containing constructs exhibited the highest expression of osteogenic genes and calcium deposition, whereas GO primarily enhanced the Young's modulus of the constructs and altered cellular morphology. In contrast, the unmodified GelMA group demonstrated superior cell proliferation at certain time points. These findings directly indicate that, within the same DLP printing system, nanomaterial-induced mechanical reinforcement and osteoinductive effects do not necessarily occur simultaneously, and different nanoparticles should therefore be selected according to their intended functional roles. Tao *et al.*[85] further employed DLP to encapsulate BMSCs within a GelMA/dextran emulsion system. The internal microvoids generated after printing improved cellular spreading, migration, and proliferation, while activating Yes-associated protein-associated signalling and ultimately enhancing bone regeneration *in vivo*. The study demonstrated that DLP not only enables precise control over macroscopic construct geometry but also regulates stem cell behaviours through bioink microstructural design.

The integration of inorganic mineral components with DLP has further expanded its applications in bone tissue engineering. Ren *et al.*[86] developed a GelMA/AlgMA/HA hybrid bioink through a one-pot fabrication strategy, enabling homogeneous incorporation of HA within the photocrosslinked polymer network. The resulting material exhibited excellent DLP printability and structural stability, while demonstrating superior bone repair outcomes compared with purely organic systems *in vivo*. In addition, multicomponent systems such as GelMA/silk methacrylate/HA have been employed for the DLP fabrication of hierarchical microporous biomimetic bone scaffolds, exhibiting enhanced tissue integration and bone regeneration capacity. Nevertheless, the compatibility of DLP with nanomaterials remains constrained by their optical properties. Increasing concentrations of nHA, CaP, GO, or other nanoparticles may alter light propagation through scattering and absorption, resulting in nonuniform photocrosslinking, reduced curing depth, or deviations between printed structures and their digital models. Therefore, in the design of nanomaterial-enhanced DLP bioinks, nanoparticle dispersion, optical absorption, photoinitiator concentration, exposure dosage, and layer thickness should be considered as interconnected design parameters rather than determining nanoparticle loading solely based on their osteogenic activity.

4. Nanomaterial-enhanced bioinks for bone tissue bioprinting

Bioinks link the fabrication process to tissue regeneration and must exhibit suitable rheological properties during printing, cytocompatibility, and sufficient structural stability after implantation.[87] However, in bone tissue engineering, mechanical performance remains a major limitation restricting the further application of cell-laden bioinks for complex bone defect repair.[88] Currently, most hydrogel-based bioinks, including GelMA, alginate, hyaluronic acid, and their composite systems, can provide extracellular matrix-like 3D microenvironments that support cell survival, proliferation, and differentiation. Nevertheless, due to their high water content and relatively low crosslinking density, their mechanical strength is generally insufficient to meet the long-term mechanical demands of load-bearing bone tissues. Therefore, the current development of nanomaterial-enhanced bioinks does not aim to simply replace conventional load-bearing implant materials, but rather to improve structural stability, mechanical properties, and tissue regenerative functions through nanoscale reinforcement while maintaining a favourable cellular microenvironment.[89,90] In recent years, various nanomaterials have been introduced into bone tissue bioprinting systems, including nHA, nanosilicates, GO, and other 2D nanomaterials. These nanoscale components can enhance the structural integrity and mechanical stability of printed bioinks by strengthening interfacial interactions within polymer networks, promoting the formation of inorganic–organic hybrid structures, and improving energy dissipation capacity.[91] Recent studies have demonstrated that the incorporation

of GO and CaP nanomaterials into GelMA systems can respectively enhance the elastic modulus and osteogenic mineralisation capacity of the constructs, indicating that different nanomaterials can provide specific regulation of the mechanical and biological properties of bioinks.[11]

The mechanisms underlying nanomaterial-enhanced bioinks extend beyond improving mechanical properties or directly promoting osteogenic differentiation, involving complex interactions between the physicochemical characteristics of materials and the cellular microenvironment. The effects of nanomaterials in bone tissue bioprinting can be classified according to their principal mechanisms of action. Nanomaterials can enhance the viscoelasticity, shear-thinning behaviour, and post-printing structural retention of bioinks through hydrogen bonding, electrostatic interactions, and interfacial interactions with polymer chains. These effects primarily influence material processability and structural stability rather than directly representing osteoinductive effects.[21] Furthermore, certain bioactive inorganic nanomaterials can regulate cellular behaviours through ion release. For example, ions released from nHA, CaP, and bioactive glass, including Ca, Si, phosphorus (P), and Sr ions, can participate in cellular signalling regulation and influence osteogenic differentiation, angiogenesis, and immune microenvironment remodelling.[92] In addition, the large specific surface area and unique surface chemistry of nanomaterials facilitate protein adsorption, biomolecule enrichment, and cell–material interactions, thereby modulating local cellular responses. Certain carbon-based and 2D nanomaterials can further influence stem cell behaviours and tissue regeneration through electrical properties, optical responses, and redox regulation.[93,94] It should be particularly emphasised that commonly used evaluation indicators, including ALP activity, osteogenic gene expression, mineral deposition, and bone formation in animal models, represent different levels of biological evidence and should not be regarded as equivalent outcomes derived from the same mechanism. Increased ALP activity mainly reflects early osteogenic differentiation trends, whereas mineral deposition and *in vivo* new bone formation more closely represent late-stage matrix maturation and tissue-level regeneration. Therefore, the evaluation of nanomaterial-enhanced bioinks should integrate material properties, underlying mechanisms, and stage-specific biological responses rather than relying solely on individual osteogenic indicators to determine regenerative capacity.[95,96]

The reinforcing effects of nanomaterials are highly dependent on nanoparticle type, size, concentration, and dispersion state. Excessive incorporation may lead to increased viscosity, reduced printability, and impaired cellular responses. Therefore, future nanomaterial-enhanced bioink design should establish a dynamic balance among mechanical reinforcement, printing performance, biological activity, and long-term biosafety rather than simply pursuing higher material stiffness. From the perspective of clinical translation, most nanomaterial-reinforced hydrogel bioinks currently remain unable to fully satisfy the requirements of large load-bearing bone defects, including mechanical strength, fatigue resistance, and long-term structural stability. Consequently, future bone tissue bioprinting strategies are more likely to adopt multimaterial synergistic approaches, in which mechanically robust polymeric, ceramic, or metallic structures provide primary mechanical support, while nanomaterial-enhanced bioinks contribute to cell delivery, osteogenic induction, and local microenvironmental regulation.[97] Recent advances in multimaterial bioprinting have enabled the spatial integration of structural supporting materials with bioactive bioinks, thereby achieving a balance between mechanical performance and tissue regenerative requirements.[97] Based on this concept, this section further systematically summarises ceramic nanomaterials, silicates and nanoclays, carbon-based nanomaterials, 2D nanomaterials, and polymeric/fibrous nanomaterials according to their material categories, with particular emphasis on how these nanomaterials improve bioink mechanical properties, printing behaviours, and bone regenerative functions through distinct mechanisms (Table 1).

4.1. Ceramic nanomaterial-enhanced bioinks

Bone extracellular matrix is composed of both organic components and highly mineralised inorganic phases, making bioceramics one of the most widely used inorganic reinforcing components in bone bioinks. When ceramic materials are reduced to the nanoscale, their specific surface area and interfacial activity are substantially increased, facilitating their dispersion within hydrogel networks and enhancing interactions with the surrounding cellular microenvironment.[98] Different ceramic systems exhibit distinct mechanisms of action. nHA possesses a high compositional similarity to native bone minerals and is primarily utilised to enhance bone-like mineral microenvironments and osteogenic activity. Amorphous calcium phosphate (ACP) and β-TCP exhibit different dissolution and phase transformation behaviours, enabling regulation of Ca- and P-mediated mineralisation processes. Bioactive glass, in contrast, can release Si, Ca, P, and dopant ions through dissolution of its glass network and can further serve as a carrier for bioactive molecule delivery through its mesoporous structure. The composition,

particle size, morphology, crystallinity, and concentration of ceramic nanoparticles collectively determine their physicochemical and biological effects within bioink systems.[99-101] Therefore, the bone regenerative effects of ceramic nanomaterials should not be simply attributed to increased expression of osteogenic markers but should be interpreted according to their specific compositions and underlying mechanisms. For nHA and CaP-based systems, their primary roles are associated with providing bone-like mineral environments, regulating Ca/P ion homeostasis, and promoting mineralisation processes, whereas bioactive glasses mainly rely on the sustained release of multiple bioactive ions and ion-mediated cellular responses that regulate osteogenic differentiation, angiogenesis, and extracellular matrix formation.

4.1.1. Hydroxyapatite nanoparticles

Hydroxyapatite is a major mineral component of native bone. Reducing HA to the nanoscale substantially increases the interfacial area between the mineral phase, hydrogel network, and surrounding cells. nHA can therefore act not only as an inorganic reinforcing phase that stabilises composite networks, but also as a source of a local Ca- and P-rich microenvironment favourable for osteogenesis and matrix mineralisation. Its influence on bioink rheology is particularly pronounced. Coşkun *et al.*[102] incorporated nHA into a chitosan-based system and systematically optimised the corresponding bioprinting parameters. The addition of nanoparticles markedly altered the rheological and printing behaviour of the material, improving the suitability of the chitosan-based formulation for 3D deposition. In a nanocellulose-based composite system, Korkeamäki *et al.*[103] progressively formulated multicomponent bioinks containing alginate, gelatin, cellulose nanofibres, and nHA. Cellulose nanofibres increased the viscosity and printability of the system, while the subsequent incorporation of nHA further improved its rheological and shape-forming properties. Following arginine–glycine–aspartic acid (RGD) functionalisation and compositional optimisation, the bioink supported long-term hBMSC viability and exhibited expression of osteogenesis-related markers, including runt-related transcription factor 2 (Runx2), osteocalcin (OCN), and ALP.

The concentration-dependent effects of nHA further demonstrate that increasing mineral content does not translate linearly into improved osteogenic performance. In GelMA/gelatin/nanocellulose bioinks containing 0, 1%, 3%, or 5% nHA, the 1% nHA formulation exhibited superior buildability and shape fidelity while maintaining high BMSC viability and metabolic activity and promoting the expression of Runx2, type I collagen, dentin matrix protein 1, and OCN. When the nHA content was increased to 5%, however, the combination of excessive viscosity and insufficient photocrosslinking compromised the long-term stability of the printed constructs and adversely affected both cell viability and osteogenic differentiation.[100] The study provides direct evidence for an optimal concentration window for nHA within bioinks and demonstrates that simply increasing mineral loading can simultaneously compromise processability and the cellular microenvironment. The physicochemical characteristics of the nanoparticles themselves represent another important but frequently overlooked design variable. Montanari *et al.*[19] compared two biomimetic Mg-doped nHA formulations. One exhibited relatively high crystallinity and a needle-like morphology, whereas the other was co-doped with Mg^{2+} and CO_3^{2-} and displayed lower crystallinity and a more rounded morphology. Both particle types were incorporated into gelatin/GelMA bioinks for hBMSC bioprinting, yet they interacted differently with the hydrogel network and produced distinct overall bioink properties. These findings indicate that even among chemically related nHA formulations, variations in crystallinity, ionic substitution, and particle morphology can substantially alter material behaviour.

Nano-hydroxyapatite can also be combined with other bioactive components to establish more complex regenerative microenvironments. Kang *et al.*[101] incorporated nHA into a composite bioink containing decellularised extracellular matrix, gelatin, and quaternised chitosan and further loaded the system with MSC-derived exosomes. The resulting bioprinted constructs simultaneously enhanced osteogenic and angiogenic processes, illustrating the evolving role of nHA from a simple mineral reinforcing phase towards an integral component of multifunctional regenerative platforms (Figure 3). Lafuente-Merchan *et al.*[18] separately incorporated HA and GO into nanocellulose-based bioinks and demonstrated that mineral particles and carbon-based nanomaterials can regulate bone regeneration-related properties through distinct mechanisms.

More broadly, studies of HA-containing bioinks also indicate a transition from simple particle incorporation towards reconstruction of a bone-like mineralised matrix. Allen *et al.*[104] incorporated 5, 10, and 20 mg/mL HA into cell-laden GelMA/gelatin bioinks and found that HA markedly reduced hydrogel swelling while increasing resistance to enzymatic degradation in a concentration-dependent manner. The groups treated with 5 or 20 mg/mL HA exhibited higher ALP activity at selected time points, whereas the 20 mg/mL HA group also showed increased *BMP7* and *BGLAP* expression without

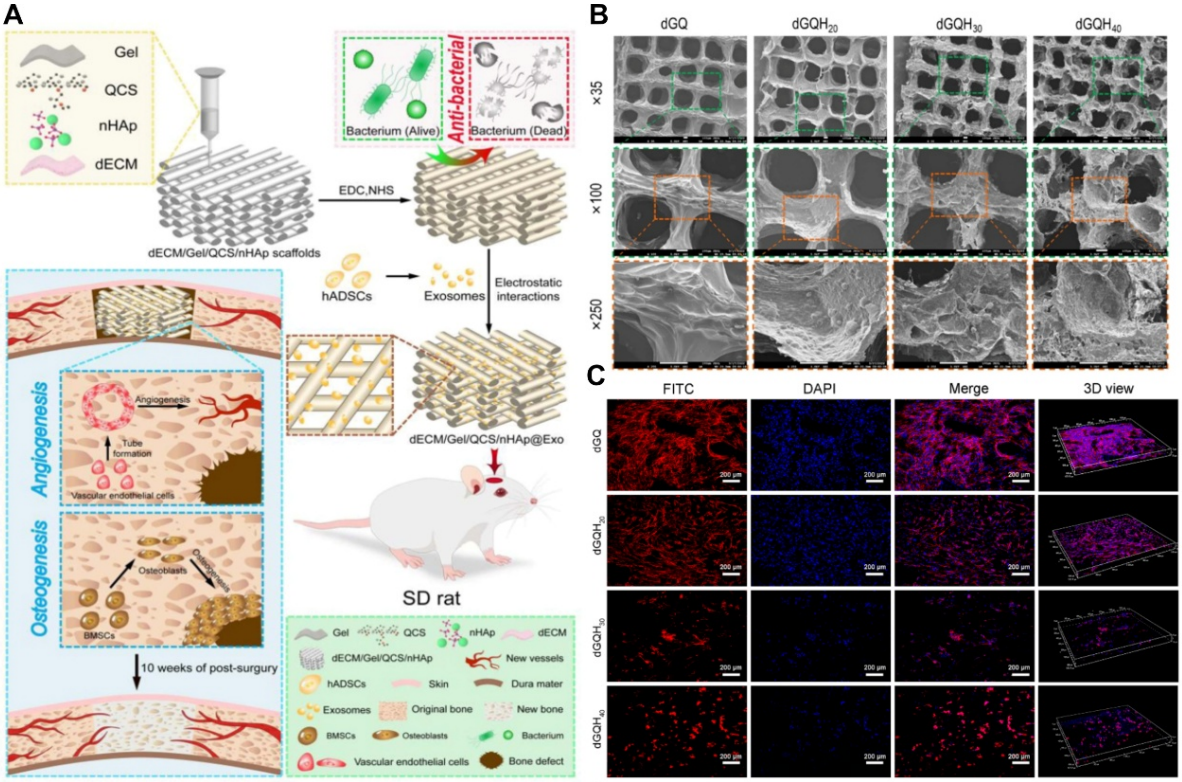


Figure 3. Nano-hydroxyapatite-containing bioinks for bioprinting-mediated bone defect repair. (A) Schematic illustration of the fabrication process and proposed regenerative mechanism of the nHAp-containing hybrid scaffold. The constructs were fabricated by 3D bioprinting using a bioink composed of dECM, Gel, QCS, and nHAp. Exosomes derived from ADSCs were subsequently incorporated into the dECM/Gel/QCS/HAp hybrid scaffolds. The resulting dECM/Gel/QCS/nHAp@Exo constructs exhibited pronounced pro-angiogenic and osteogenic activity together with antibacterial properties, thereby accelerating bone defect repair. (B) Representative scanning electron microscopy images of the nHAp-containing hybrid scaffolds. (C) Representative cytoskeletal staining images of cells cultured within the nHAp-containing hybrid scaffolds. Figure reprinted with permission from Kang *et al.*[101] Copyright © 2023 IOP.

Abbreviations: BMSCs: Bone marrow-derived mesenchymal stem cells; DAPI: 4′,6-diamidino-2-phenylindole; dECM: Decellularised extracellular matrix; EDC: 1-Ethyl-3-(3-dimethylaminopropyl)carbodiimide; FITC: Fluorescein isothiocyanate; Gel: Gelatin; hADSCs: Human adipose-derived stem cells; nHAp: Nano-hydroxyapatite; NHS: *N*-hydroxysuccinimide; QCS: Quaternized chitosan; SD: Sprague–Dawley.

substantially compromising cell viability or proliferation. Wang *et al.*[8] further developed large-scale self-mineralising bone organoids using a GelMA/AlgMA/HA hybrid bioink (Figure 4A). By providing a biomaterial environment capable of recapitulating key structural and functional features of native mineralised bone, this system enabled the bioprinted constructs to undergo sustained maturation and progressively establish a bone-like mineralised microenvironment during long-term culture (Figure 4B), ultimately resulting in enhanced bone regenerative capacity both *in vitro* and *in vivo* (Figure 4C). In the same year, Ren *et al.*[86] developed a HA-containing hybrid bioink through a one-pot strategy for DLP fabrication, further supporting the emerging shift from simple HA particle addition towards the cooperative construction of mineralised matrices through interactions between the inorganic phase and hydrogel network. It should be noted, however, that HA in several of these latter studies was not explicitly defined as nanoscale. These findings should therefore be regarded as complementary evidence for the broader evolution of HA-based bioink design rather than as direct evidence for nHA-specific effects.

The advantages of nHA ultimately depend on an appropriate particle concentration and stable dispersion within the bioink. Although its high specific surface area enhances material–cell interactions, it also increases the propensity for particle aggregation and interference with polymer network formation. In photocrosslinkable bioinks, nHA can additionally induce substantial light scattering and thereby reduce crosslinking uniformity. Future studies should therefore move beyond comparisons of nHA concentrations to systematically investigate particle size, aspect ratio, crystallinity, surface modification, and ionic substitution. These parameters should be evaluated in conjunction with the printing process to determine their

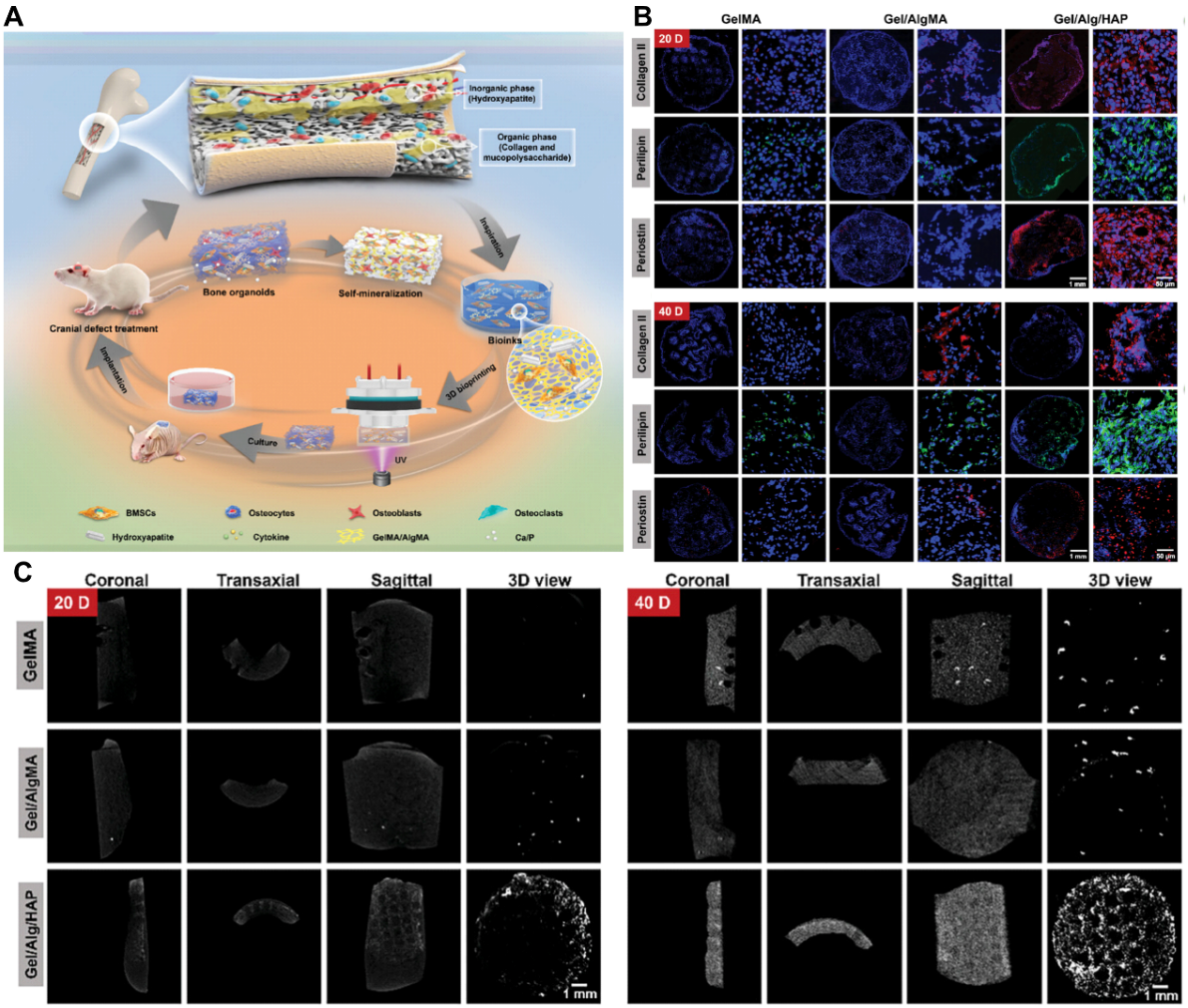


Figure 4. Large-scale bioprinted self-mineralising bone organoids constructed using an HAP-hybrid bioink. (A) Schematic illustration of the overall study design and experimental workflow for the fabrication and evaluation of bioprinted self-mineralising bone organoids. (B) Micro-computed tomography reconstructions of the bioprinted self-mineralising bone organoids after 20 and 40 days of *in vitro* culture, showing the progressive development of mineralised tissue within the constructs. (C) *In vivo* evaluation of bioprinted GelMA, GelMA/AlgMA, and GelMA/AlgMA/HAP constructs. The GelMA/AlgMA/HAP hybrid bioink supported the formation of bioprinted bone organoids with multicellular differentiation and enhanced bone tissue development. Figure reprinted with permission from Wang *et al.*[8] Copyright © 2024 Wiley-VCH GmbH.
Abbreviations: Alg: Alginate; AlgMA: Methacrylated alginate; BMSCs: Bone marrow-derived mesenchymal stem cells; CaP: Calcium phosphate; Gel: Gelatin; GelMA: Gelatin methacryloyl; HAP: Hydroxyapatite; UV: Ultraviolet.

combined effects on construct stability, cellular responses, and long-term osteogenic performance.

4.1.2. Calcium phosphate nanoparticles

From a compositional perspective, HA itself belongs to the CaP family. Given the comparatively large body of research on nHA in bone bioprinting, it is discussed separately above, whereas this section focuses primarily on ACP, β-TCP, and other non-HA CaP nanophases. Compared with relatively stable HA, different CaP phases exhibit substantial variations in crystallinity, solubility, and phase-transformation behaviour, providing a broader design space for regulating bioink mineralisation and the local ionic microenvironment.

In situ formation of CaP within hydrogel networks offers a potential strategy for reducing the heterogeneous dispersion associated with preformed particles. Bhattacharyya *et al.*[105] generated CaP microparticles and nanoparticles directly within a GelMA system and tuned the mean particle size from approximately 1.753 μm to 296 nm by varying the gelatin concentration. Incorporation of CaP increased the compressive strength to approximately 3 times that of pristine GelMA and enabled the fabrication of self-supporting constructs exceeding 2 cm in height

and approximately 160 layers, while also enhancing osteogenesis-related cellular responses. The study demonstrates that CaP does not function solely as a bioactive mineral phase. Its mode of formation and particle dimensions can also directly modulate the rheological and mechanical properties of the bioink. The osteogenic contribution of CaP has also been demonstrated more directly in cell-laden photocrosslinkable systems. Kühl *et al.*[11] separately incorporated CaP and GO into GelMA for DLP bioprinting. Although cells in the unmodified GelMA group exhibited favourable proliferation, the CaP-containing constructs produced the strongest osteogenic response in hMSCs, including more pronounced osteogenic gene expression and calcium deposition, whereas GO predominantly increased the elastic modulus. This comparison highlights the material-specific functions of nanomaterials within bioinks. In bone bioprinting, enhanced structural stiffness and enhanced cellular osteogenesis are therefore not necessarily achieved by the same particulate component.

Beta-tricalcium phosphate provides another route for exploiting CaP-mediated regulation. Zhang *et al.*[68] incorporated nano-β-TCP together with osteogenic cells into the outer GelMA/alginate layer of a triaxial bioprinting system, while HUVECs were positioned within the intermediate layer and a sacrificial inner layer was used to generate a continuous channel. This configuration produced a tissue-engineered bone model with spatially distinct osteogenic and vascular compartments. The study suggests that CaP nanophases do not need to be uniformly distributed throughout an entire construct. Instead, multimaterial printing can localise nano-β-TCP within specific regions, enabling clearer spatial partitioning between mineral-mediated osteogenic induction and vascular microenvironmental regulation. ACP, owing to its amorphous structure and comparatively high reactivity, has also begun to attract attention in emerging bioink formulations. Indurkar *et al.*[106] incorporated ACP into an alginate dialdehyde/gelatin (ADA-GEL) system to develop an ACP-reinforced ADA-GEL bioink for bone tissue biofabrication. Such approaches extend CaP-based bioinks beyond stable crystalline particles towards amorphous mineral phases capable of subsequent transformation.

Earlier β-TCP printing studies also provide useful evidence regarding the relationship between CaP loading and bioink performance. Incorporation of β-TCP substantially increased the viscosity of alginate-based formulations, while a 10% alginate/β-TCP system enhanced both MG-63 cell proliferation and ALP activity.[107] However, because the study involved an acellular printed scaffold and did not explicitly define β-TCP as nanoscale, it should primarily be regarded as supporting evidence for the concentration-dependent effects of CaP on material performance rather than as direct evidence for cell-laden nanoCa–P bioprinting.

The principal advantage of CaP nanomaterials lies in their combination of mineral biomimicry with tunable dissolution and phase transformation, although these features also introduce greater complexity in material control than is generally encountered with nHA. CaP phase composition, Ca/P ratio, crystallinity, and particle size can collectively alter ion release, mineralisation kinetics, and hydrogel stability. In photocrosslinkable systems, particle-induced light scattering may reduce curing depth, whereas in extrusion-based systems, high solid contents can substantially alter viscosity and pressure requirements. Future CaP-enhanced bioinks should therefore move beyond simple comparisons between formulations with and without CaP and instead focus on controlling mineral phase, particle dimensions, and spatial distribution so that dissolution behaviour can be matched more closely to cellular osteogenesis and matrix mineralisation.[68]

4.1.3. Bioactive glass nanoparticles

Bioactive glass nanoparticles differ fundamentally from HA and conventional CaP particles because of their amorphous glass networks and pronounced capacity for ion release. Glass composition can be tailored by varying the proportions of Si, Ca, and P or by incorporating therapeutic elements such as Cu, zinc (Zn), and Sr. MBGNs further provide high specific surface areas and pore volumes, creating additional opportunities for controlled ion release and loading of bioactive molecules. Following exposure to aqueous environments, the glass network progressively dissolves, meaning that the biological activity of BGNs depends more strongly on dynamic ion exchange than on the long-term persistence of a stable mineral phase. BGN-enhanced bioinks can therefore combine rheological regulation with biologically active ion delivery.

Zhu *et al.*[9] incorporated aminated Cu-doped mesoporous BGNs into a dynamic covalent network formed from alginate dialdehyde and gelatin, thereby developing a nanocomposite bioink suitable for extrusion-based bioprinting. The MBGNs improved rheological behaviour, shape fidelity, and post-printing structural stability while supporting cell proliferation and spreading and enhancing osteogenic differentiation. A notable feature of this system is that the glass nanoparticles contributed both to the formation of the composite network and to biological functionality through the ionic activity of Cu and the glass matrix, representing a transition from BGNs as passive inorganic reinforcing phases towards multifunctional

nanoscale components. Bhattacharyya *et al.*[108] incorporated BGNs into alginate/agarose bioinks and further modulated the system using essential trace elements including iron, Zn, and Cu. Increasing BGN content improved hydrogel pore characteristics, compressive and cyclic mechanical performance, and 3D printability. Culture experiments with adipose-derived MSCs and MC3T3 cells further demonstrated enhanced cell growth and extracellular matrix formation with increasing bioactive glass content.

Mesoporous bioactive glass nanoparticles can also be incorporated into photocrosslinkable systems. In 2024, Sánchez-Rodríguez *et al.*[109] dispersed mesoporous BGNs within GelMA and used a low-cost light-based bioprinting platform to fabricate cell-laden constructs. The system achieved a printing resolution of approximately 250 μm, maintained cell viability above 85% after several weeks of culture, and supported C2C12 cell spreading, alignment, and tissue maturation. As with other nanomaterial-enhanced bioinks, however, glass concentration requires careful control. Kolan *et al.*[110] incorporated rapidly dissolving borate bioactive glass at concentrations ranging from 0.075% to 0.6% into an alginate/gelatin system. Although glass incorporation increased hydrogel stiffness, different concentrations produced distinct effects on the early cellular state of human adipose-derived MSCs.

Compared with nHA, the major advantage of BGNs lies in their compositional tunability and capacity for multifunctional ion release, yet these same characteristics also increase formulation complexity. Glass composition, mesoporous architecture, and particle loading collectively influence dissolution kinetics and the resulting cellular exposure to released ions. A given functional ion may promote osteogenesis or angiogenesis within an appropriate concentration range, whereas excessively rapid release can induce local cellular stress. Evaluation of BGN-enhanced bioinks should therefore extend beyond initial post-printing mechanical properties and short-term cell viability to include quantitative assessment of ion-release kinetics, long-term structural evolution, and osteogenic responses. Existing studies demonstrate that BGNs can integrate printability with biological functionality, but establishing quantitative relationships among glass composition, released ion dose, and bone regenerative outcomes remains a key challenge for future bioink design.[9,108]

4.2. Silicate and nanoclay-enhanced bioinks

Silicates and nanoclays have gradually emerged as important inorganic functional components in bone tissue bioinks due to their high specific surface area, abundant surface charges, and excellent aqueous dispersibility.[111] Unlike nHA and CaP, which primarily mimic the mineral composition of native bone, these materials not only contribute to the construction of inorganic microenvironments but also significantly regulate hydrogel rheological behaviour and structural stability through reversible interactions between particles and polymer chains.[112] Certain silicate-based materials can release bioactive ions, including Si, Ca, and Mg, during degradation, thereby further modulating osteogenesis, angiogenesis, and neuro-related cellular behaviours. Nanoclays exhibit strong adsorption capacity and can interact with proteins, growth factors, and small-molecule drugs, thereby providing both rheological regulation and localised delivery functions.[113] The size, morphology, layered structure, and ionic composition of different materials determine their predominant roles within bioink systems; therefore, their physical reinforcement and biological activation effects should be carefully distinguished. Specifically, the biological effects of silicate materials are primarily associated with soluble ion release and subsequent signalling regulation, whereas the advantages of nanoclays are largely derived from their ability to modulate rheological properties, provide surface adsorption sites, and facilitate the delivery of bioactive molecules such as growth factors. Therefore, enhanced osteogenic outcomes observed in these systems may result from the combined effects of optimised material properties and regulation of the cellular microenvironment rather than from a single direct osteoinductive mechanism.

4.2.1. Nanosilicates

Silicate nanomaterials can regulate cellular behaviours through the release of soluble silicon and other accompanying ions, with Si-associated signalling being widely investigated for promoting osteogenic differentiation, matrix mineralisation, and vascular-related responses. However, the mineralisation enhancement induced by silicate materials does not necessarily represent direct stimulation of osteogenic differentiation. In addition to Si-mediated signalling regulation, released ions may indirectly promote bone formation by improving the angiogenic microenvironment. Unlike conventional growth factors, inorganic silicate nanophases can directly serve as structural components within bioinks, enabling the simultaneous regulation of material properties and biological activity within a single system. Furthermore, their nanoscale dimensions increase the interfacial contact area with hydrogel networks and encapsulated cells, allowing significant modulation of bioink rheological properties and cellular responses even at relatively low incorporation levels.

The NICE bioink developed by Chimene *et al.*[14] represents a landmark example of this strategy. The system consisted

of GelMA, κ-carrageenan, and 2D nanosilicate particles. Reversible physical interactions between the nanosilicates and polymer chains improved shear-thinning behaviour and printing stability while simultaneously imparting osteoinductive activity to the construct. Bioprinted hMSCs maintained long-term viability and exhibited enhanced osteogenic differentiation and mineralisation. Importantly, the study established nanosilicates not merely as fillers for increasing material stiffness, but as functional components capable of simultaneously regulating rheological behaviour and cell fate, thereby enabling the development of bone bioinks that combine printability with biological activity. Liu *et al.*[15] subsequently incorporated nanosilicates into a cell-laden gelatin/alginate bioink for the repair of critical-sized calvarial defects in rats. Nanosilicate incorporation markedly improved shear-thinning behaviour and compressive properties. In particular, 2% nanosilicate increased the compressive modulus from approximately 47 to 101 kPa and enabled stable printing of constructs up to 15 mm in height. Encapsulated BMSCs exhibited enhanced osteogenic marker expression and mineralisation, while implantation into calvarial defects resulted in increased new bone formation.

More recently, nanosilicate-based bioinks have progressed beyond the direct promotion of osteogenesis towards coordinated regeneration involving multiple tissue components. Zhang *et al.*[114] incorporated calcium silicate nanowires with diameters of approximately 10–50 nm into GelMA and combined the formulation with BMSCs and Schwann cells to construct a hierarchically organised neuro-osseous bioprinted system (Figure 5A). The calcium silicate nanowires supported long-term survival and spreading of encapsulated cells while simultaneously enhancing osteogenic differentiation of BMSCs and neural-related cellular phenotypes (Figure 5B). In a critical-sized rat calvarial defect model, the calcium silicate nanowire-containing neuro-osseous constructs promoted both new bone formation and nerve fibre ingrowth (Figure 5C). Silicate materials have also begun to be used for modulation of the bone immune microenvironment. Yu *et al.*[33] incorporated Sr-doped calcium silicate hydrate into GelMA containing BMSCs to develop a bioink with combined immunomodulatory and osteogenic functions. The system regulated macrophage-associated immune responses while enhancing BMSC osteogenic differentiation and produced substantial bone regeneration in a critical-sized defect model, with the optimised formulation reported to achieve nearly complete defect repair. Compared with earlier strategies that primarily relied on Si-mediated stimulation of osteogenesis, these studies extend the function of silicate materials towards regulation of the host immune microenvironment.

These developments indicate that silicate-enhanced bioinks are evolving from simple material reinforcement towards ion-mediated regulation of multiple cell populations and regenerative processes. The concentrations and release kinetics of Si, Ca, Sr, and other ions may simultaneously influence osteogenic, vascular, neural, and immune responses, and the biological effects of silicates should therefore not be reduced to a generic promotion of osteogenesis. Excessive particle loading may also increase bioink viscosity to unfavourable levels and alter crosslinking behaviour and the local cellular microenvironment. Future studies should establish more quantitative relationships among silicate composition, particle morphology, ion-release kinetics, and specific cellular responses to define appropriate dose windows for their use as active components of bone bioinks.

4.2.2. Nanoclays

Nanoclays typically possess layered, plate-like, or rod-like nanostructures, with Laponite and ATP representing two commonly investigated examples. Their surfaces carry abundant exchangeable charges that can establish reversible physical interactions with gelatin, GelMA, alginate, and other polymers, thereby exerting pronounced effects on bioink viscosity, yield stress, and shear-thinning behaviour. Compared with most ceramic nanoparticles, the principal advantage of nanoclays does not lie primarily in increasing the mineral content of the construct. Instead, they combine rheological regulation with ion release and biomolecular adsorption. Certain nanoclays can also adsorb growth factors and attenuate their initial burst release, thereby integrating material reinforcement with localised therapeutic delivery.

Cidonio *et al.*[43] reported a systematic application of nanoclay-based bioinks for bone tissue bioprinting. BMSCs encapsulated within the nanoclay bioink maintained high viability over 21 days of culture and formed pronounced mineralised tissue under osteogenic conditions. The material also served as a carrier for VEGF and bone morphogenetic protein 2 (BMP-2). When combined with HUVECs and VEGF, the printed constructs induced substantial vascular ingrowth in the chick chorioallantoic membrane model. BMP-2-loaded printed scaffolds generated significantly more mineralised tissue after four weeks *in vivo* than BMP-2-free and alginate controls, while BMSC-laden-printed constructs likewise produced more bone tissue than acellular and non-printed controls. Laponite has subsequently been exploited to recapitulate neuroregulatory features of the bone regenerative microenvironment. Li *et al.*[115] adsorbed nerve growth factor (NGF) onto Laponite and incorporated the resulting complex into a cell-laden GelMA/AlgMA bioink (Figure

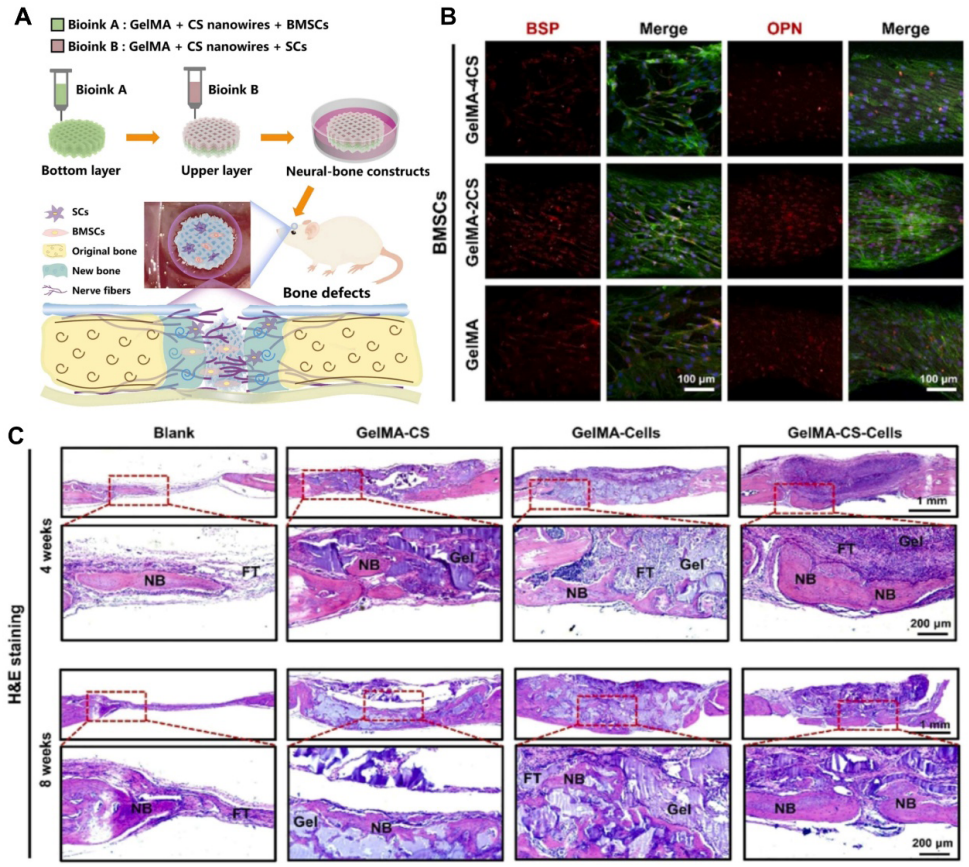


Figure 5. Silicate-enhanced bioinks for bioprinting-mediated bone repair. (A) Schematic illustration of the fabrication of a 3D-bioprinted neuro-osteogenic construct and its application in nerve-guided bone regeneration. During bioink preparation, inorganic CS nanowires, SCs, and BMSCs were incorporated into a GelMA hydrogel. The neuro-osteogenic constructs were then fabricated by multicellular 3D bioprinting. Following implantation into bone defects, the bioactive CS nanowires and encapsulated cells synergistically promoted bone regeneration and nerve fibre ingrowth, thereby enabling effective nerve-guided bone regeneration. (B) Immunofluorescence images showing OPN expression in BMSCs within the 3D-bioprinted neuro-osteogenic constructs. (C) H&E staining images of newly formed bone tissue in each group at 4 and 8 weeks. The 3D-bioprinted GelMA-CS-Cells group exhibited significantly improved bone regeneration, indicating a pronounced synergistic effect of the CS nanowires and encapsulated cells. In addition, the newly formed bone tissue integrated well with the constructs and surrounding host tissue. Figure reprinted with permission from Zhang *et al.*[114] Copyright © 2022 Elsevier Ltd. Abbreviations: BMSCs: Bone marrow-derived mesenchymal stem cells; BSP: Bone sialoprotein; CS: Calcium silicate; FT: Fibrous tissue; Gel: Gel/hydrogel; GelMA: Gelatin methacryloyl; H&E: Hematoxylin and eosin; NB: New bone; OPN: Osteopontin; SCs: Schwann cells.

6A). Laponite prolonged local NGF release while also contributing to the regulation of sensory nerve-related signalling. *In vitro*, NGF@Laponite promoted axonal extension and calcitonin gene-related peptide-associated neural responses and enhanced BMSC osteogenesis through neuro-osseous signalling (Figure 6B). Following implantation into calvarial defects, NGF@Laponite-containing constructs promoted the formation of more abundant neurovascular networks, enhanced BMSC osteogenic differentiation, and increased new bone formation within the defect region (Figure 6C).

The structural contribution of Laponite has also been exploited for the repair of complex bone defects. Yang *et al.*[116] developed a composite hydrogel composed of GelMA, Laponite, and *N*-acryloyl glycinamide and fabricated hollow structures using coaxial printing. The material exhibited pronounced elastic recovery and fatigue resistance, enabling large numbers of cells to be rapidly loaded into the constructs through cyclic compression. Compared with static cell loading, the mechanically assisted strategy markedly increased cellular infiltration within several seconds and enabled spatially selective loading of different cell populations. Constructs containing BMSCs alone or BMSCs together with endothelial cells enhanced both bone repair and vascularisation in rat segmental and osteoporotic bone defect models. The naturally occurring rod-like nanoclay ATP has likewise shown considerable potential for bone bioprinting. Liu *et al.*[10] incorporated nano-ATP into GelMA and directly

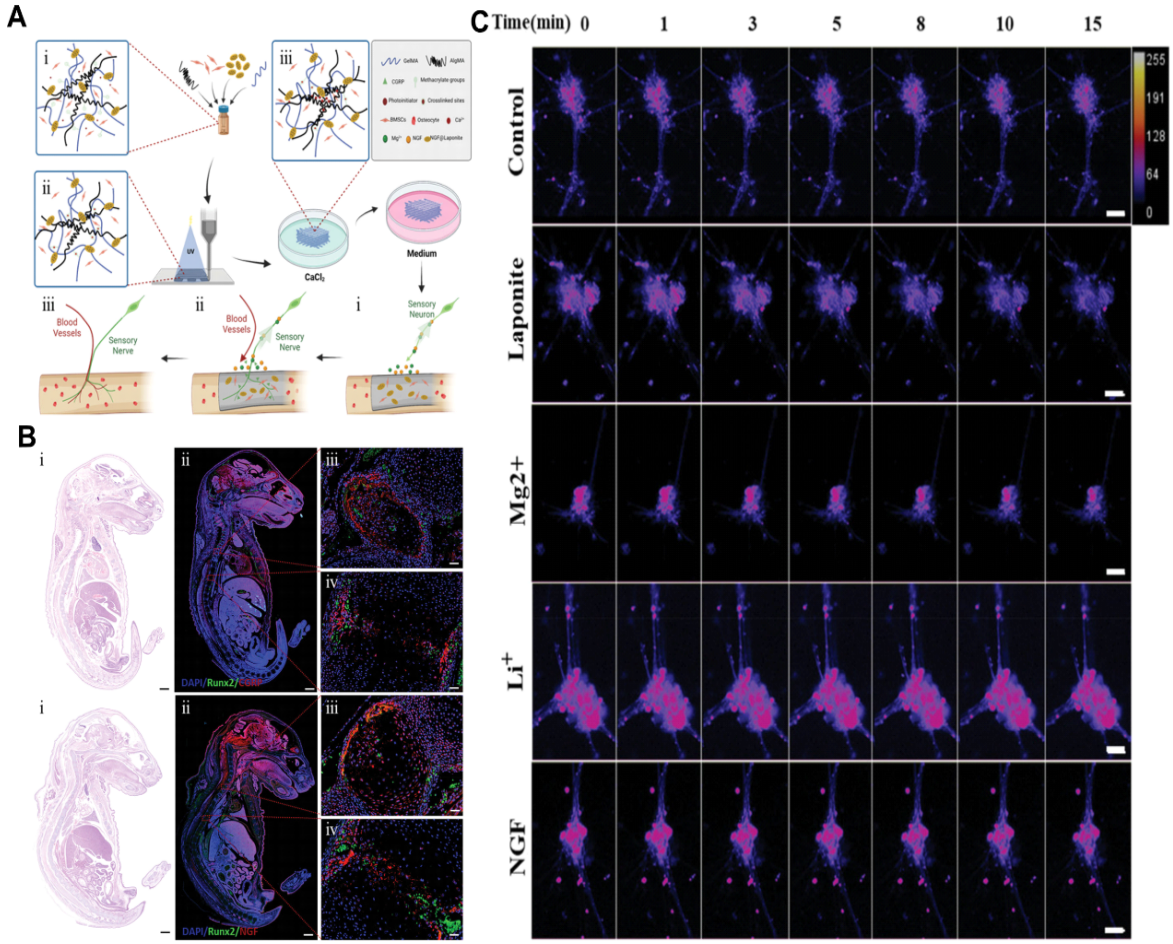


Figure 6. Laponite-based bioprinted constructs mimic the ossification centre microenvironment to promote targeted innervation and bone regeneration. (A) Schematic illustration of the fabrication strategy of Laponite-based bioprinted constructs using Laponite, AlgMA, and GelMA bioinks to generate an ossification-centre-mimicking microenvironment. (B) Immunofluorescence characterisation of neurogenic and osteogenic signalling molecules in the embryonic ossification centre. Runx2 (green) was used as an osteogenic marker, while CGRP and NGF (red) represented sensory nerve-related signals. (C) Time-lapse fluorescence imaging demonstrating the effects of different bioink components on synaptic vesicle exocytosis in dorsal root ganglia (DRG)-derived neurons. Figure reprinted with permission from Li *et al.*[115] Copyright © 2021 Wiley-VCH GmbH.
Abbreviations: AlgMA: Alginate methacrylate; BMSCs: Bone marrow-derived mesenchymal stem cells; CGRP: Calcitonin gene-related peptide; DAPI: 4′,6-Diamidino-2-phenylindole; GelMA: Gelatin methacryloyl; NGF: Nerve growth factor; Runx2: Runt-related transcription factor 2; UV: Ultraviolet.

encapsulated BMSCs for bioprinting. The nanoparticles improved printability and mechanical stability while promoting osteogenic differentiation of BMSCs. When evaluated using endothelial cells, the nano-ATP composite hydrogel also exhibited enhanced angiogenic activity. In a rat calvarial defect model, cell-laden nano-ATP/GelMA constructs significantly increased both new bone formation and vascularisation. Rather than merely improving material strength, the study more directly demonstrates that ATP can simultaneously regulate osteogenic and angiogenic processes. The ionic composition of ATP can be further modified to tune its biological activity. Liu *et al.*[117] incorporated Sr into nano-ATP and developed a Sr-ATP/GelMA/chitosan composite hydrogel for 3D bioprinting. Comparison of 0.5%, 1.0%, and 2.0% Sr-ATP revealed clear concentration-dependent differences in material properties and cellular responses. The optimised formulation exhibited superior osteogenic and angiogenic activity and further improved bone defect repair.

Following the fabrication of Gel/SA/nano-ATP scaffolds, BMSCs were subsequently seeded onto the printed constructs, and new bone formation was observed at 12 weeks in a rabbit tibial plateau defect model.[118] Although the study demonstrates the beneficial effects of nano-ATP on rheological properties, mechanical performance, and bone regeneration, it is more accurately classified as a 3D-printed biomaterial scaffold rather than cell-laden bioprinting. The primary advantage of nanoclays

lies in their multifunctionality, as a single material can simultaneously contribute to bioink rheological regulation, mechanical stability, biological activity, and molecular delivery. However, these functions are also closely interconnected. Increasing the nanoclay concentration generally enhances yield stress and shape fidelity but may also increase extrusion resistance and restrict cell migration. Similarly, their strong protein adsorption capacity can facilitate the sustained release of growth factors while potentially altering the effective concentrations of proteins in the culture medium and cell-secreted factors. Therefore, increased ALP expression or mineralisation in nanoclay-based systems should be interpreted as the combined outcome of material-mediated structural regulation, ion release, and biomolecular delivery, rather than as direct evidence of a single osteogenic mechanism.

4.3. Carbon-based nanomaterial-enhanced bioinks

Carbon-based nanomaterials possess high specific surface areas, tunable surface chemistry, and pronounced interfacial activity, enabling them to modulate the rheological, mechanical, and biological properties of bioinks through interactions with hydrogel networks and extracellular proteins. Unlike ceramic and silicate nanomaterials, whose biological effects are largely associated with mineral composition or ion release, the functions of carbon-based materials are closely related to their carbon framework, surface functional groups, electrical properties, and optical responsiveness.[16] GO contains abundant oxygen-containing functional groups and exhibits considerably better aqueous dispersibility than pristine graphene. Consequently, current research on carbon-based materials for bone bioprinting has focused predominantly on GO, whereas direct incorporation of non-oxidised graphene into cell-laden bioinks remains relatively limited.[119] Carbon quantum dots (CQDs), by contrast, are characterised by their ultrasmall dimensions, favourable aqueous dispersibility, readily functionalised surfaces, and intrinsic fluorescence, and may additionally serve as platforms for drug delivery, photoresponsive regulation, and immunomodulation.[120,121] These characteristics indicate that the effects of carbon-based nanomaterials are strongly dependent on concentration and surface chemistry, and that improvements in mechanical performance, cell proliferation, and osteogenic differentiation do not necessarily occur in parallel.

4.3.1. Graphene and graphene oxide

Graphene is a 2D material composed of sp^2-hybridised carbon atoms and possesses exceptional mechanical and electrical properties. However, its hydrophobicity and tendency to aggregate in aqueous environments restrict its direct incorporation into cell-laden bioinks. GO has therefore been investigated more extensively than pristine graphene in bone tissue bioprinting. Its principal functions include modulation of bioink rheology and mechanical properties, together with regulation of stem-cell proliferation, osteogenic differentiation, and matrix mineralisation.

Zhang *et al.*[16] systematically investigated the concentration-dependent effects of GO in cell-laden bone bioinks. GO at concentrations of 0.5, 1, and 2 mg/mL was incorporated into an alginate/gelatin system containing hMSCs for extrusion-based bioprinting. GO addition improved printability, structural fidelity, and early compressive properties. Among the tested formulations, the 1 mg/mL GO group exhibited the most pronounced long-term osteogenic response, with increased expression of osteogenesis-related genes including *ALPL*, *BGLAP*, and *PHEX* and the greatest mineralised tissue volume after 42 days. In contrast, increasing GO to 2 mg/mL resulted in pronounced construct swelling during prolonged culture and produced the lowest compressive modulus at day 42. The 1 mg/mL formulation also better preserved the geometry of printed defect-like constructs. These findings demonstrate that the optimal GO concentration cannot be defined solely on the basis of initial mechanical reinforcement, as long-term structural behaviour and osteogenic performance may follow different concentration-dependent trends.

Jiang *et al.*[122] directly incorporated GO together with MSCs into GelMA for bioprinting. GO addition did not substantially compromise printing performance or cell viability and simultaneously promoted MSC proliferation. Following osteogenic induction, GO-containing constructs exhibited higher ALP activity and increased expression of osteogenic genes and proteins, including osteopontin, OCN, and Runx2. GO can also be combined with nanocellulose systems that provide stronger rheological regulation. Lafuente-Merchan *et al.*[18] separately incorporated HA and GO into nanocellulose/alginate bioinks to compare the effects of mineral and carbon-based components on bioprinted bone constructs. Both additives reduced the structural alterations observed in the unmodified nanocellulose/alginate system during long-term culture, while the GO-containing formulation exhibited favourable osteogenic differentiation. These findings illustrate the potential of combining GO with fibrous nanoscale networks to create multiscale composite bioinks, in which carbon-based nanosheets predominantly modulate interfacial and biological functions while nanocellulose provides the principal rheological and structural support. Importantly, however, the osteogenic

effects of GO are not consistent across all bioink formulations. Kühl *et al.*[11] directly compared GO- and CaP-modified GelMA using DLP bioprinting. GO increased the Young's modulus of the constructs and markedly altered hMSC morphology, whereas the CaP-containing group exhibited the highest osteogenic gene expression and calcium deposition. Unmodified GelMA also supported superior cell proliferation at selected time points. These results reinforce the concept that the biological function of GO is highly dependent on the surrounding polymer network, concentration, printing modality, and the specific outcome being evaluated. Mechanical reinforcement by GO should therefore not be assumed to translate directly into enhanced osteogenic differentiation.

Similar to other nanomaterial systems, the application of GO also faces several critical limitations. Increasing GO sheet concentration may enhance water absorption and promote aggregation, while simultaneously altering the viscosity and crosslinking behaviour of bioink networks. The size, oxidation degree, and density of surface functional groups of GO vary considerably among different studies, and these parameters may significantly influence protein adsorption, cellular internalisation, and long-term biocompatibility. For photopolymerisation-based approaches such as DLP, the intrinsic light absorption capacity of GO may further interfere with the photochemical crosslinking process. Therefore, the contribution of GO to bone regeneration is more likely associated with interfacial regulation, protein adsorption, and optimisation of the mechanical microenvironment, whereas its effects on osteogenic differentiation may depend on the combined modulation of cell–material interactions mediated by these factors.

4.3.2. Carbon quantum dots

Carbon quantum dots typically consist of carbonaceous cores only a few nanometres in size surrounded by surfaces rich in functional groups. Their dimensions are substantially smaller than those of GO nanosheets, and they generally exhibit favourable aqueous dispersibility and tunable photoluminescence. CQD surfaces can be further modified with nitrogen- or oxygen-containing groups and other functional moieties, enabling their use in cell tracking, biomolecular delivery, photoresponsive regulation, and modulation of cellular behaviour[120] Their potential role in bone bioinks therefore differs fundamentally from that of GO. Whereas GO primarily serves as a structural and interfacial modifier within composite networks, CQDs are better suited to function as nanoscale carriers and regulators of biological signalling. At present, direct studies incorporating CQDs into cell-laden bone bioinks remain relatively limited, although their application is beginning to expand from osteogenic stimulation towards immunomodulation, antitumour therapy, and infection control for the treatment of complex bone defects.

Dutta *et al.*[121] incorporated 100 μg/mL polyphenol-derived CQDs into 12 wt% GelMA to develop an extrusion-printable GelMA/CQD nanocomposite bioink with additional photoresponsive drug-delivery functionality. The formulation maintained favourable rheological and printing properties and was used to fabricate 3D constructs containing BMSCs and vascular-associated cells (Figure 7A). The CQD-containing system promoted macrophage transition towards a repair-associated phenotype, and the resulting conditioned microenvironment further enhanced osteogenesis in BMSCs while supporting angiogenic responses. Near-infrared irradiation additionally exploited the photoresponsive properties of the CQDs to provide an antitumour effect against bone malignancy. In a rat calvarial defect model, the printed constructs promoted bone regeneration within the defect region. The study illustrates how CQDs can integrate immunomodulatory, osteogenic, angiogenic, and externally triggered therapeutic functions within a single bioprinted platform.

Bu *et al.*[123] synthesised osteoactive carbon dots from ascorbic acid and polyethyleneimine and exploited their surface functionality to deliver miR-2861. The carbon dots themselves increased ALP activity and mineralisation in BMSCs, while miR-2861 loading further enhanced osteogenic differentiation and produced a synergistic increase in new bone formation *in vivo*. From a bioprinting perspective, such properties suggest that CQDs could provide a means of incorporating gene-regulatory or small-molecule signals into cell-laden bioinks with high spatial precision. However, the study did not itself employ bioprinting and should therefore be regarded as mechanistic support for the design of functionalised CQD-containing bioinks rather than as direct evidence of CQD-assisted bioprinting.

The surface chemistry of CQDs can also be tailored to address the multiple pathological features associated with complex bone defects. Geng *et al.*[124] demonstrated that altering CQD surface charge markedly changed their biological functions. Positively charged CQDs predominantly exhibited antibacterial and antibiofilm activity against multidrug-resistant bacteria, whereas negatively charged CQDs exerted more pronounced pro-regenerative effects on bone. The two CQD populations were subsequently integrated into GelMA hydrogels, which achieved a new bone area of 97.0 ± 1.6% at 60 days in a methicillin-resistant *Staphylococcus aureus*-infected calvarial defect model. Near-infrared-responsive carbon

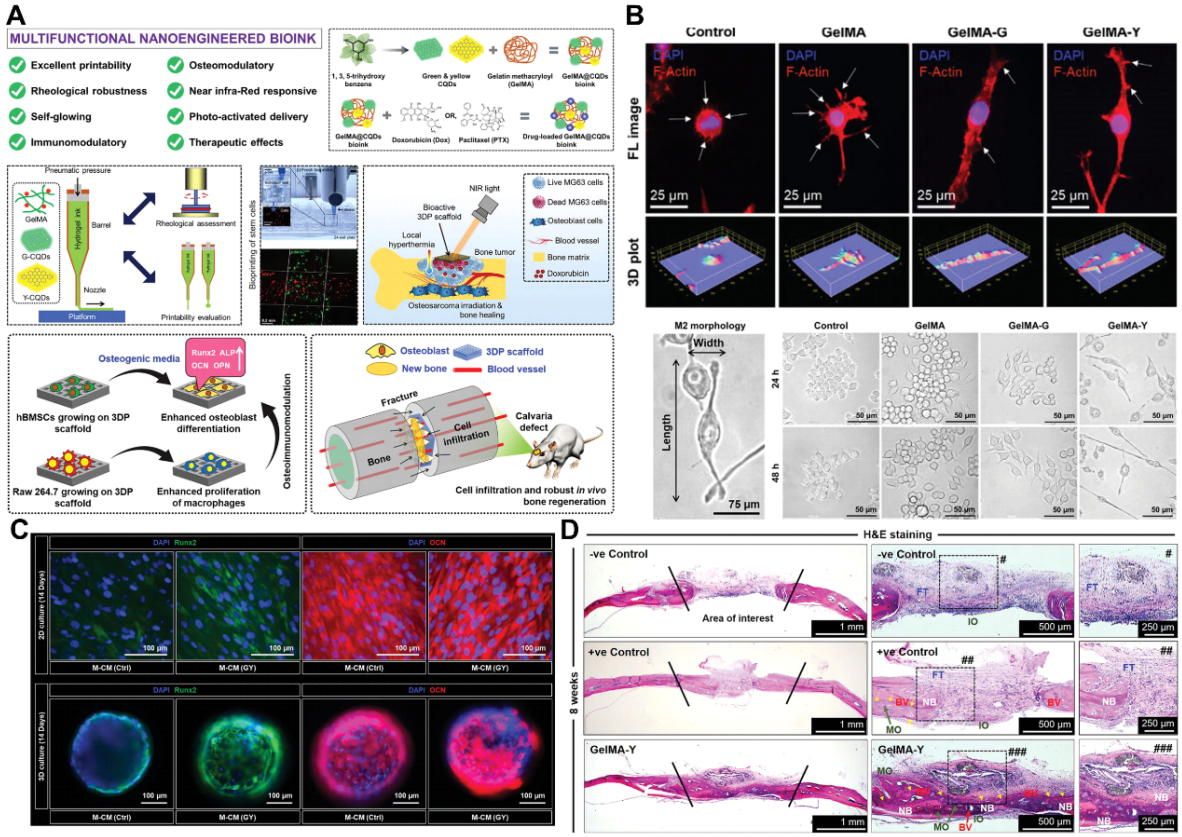


Figure 7. CQD-enhanced bioinks for bioprinting-mediated bone repair. (A) Schematic illustration of the mechanism by which polyphenol-derived CQD-incorporated composite scaffolds promote tissue repair and regeneration. (B) Representative FL microscopy images of RAW 264.7 cells showing actin organisation and branching patterns, together with corresponding optical microscopy images showing the M2-like macrophage differentiation features of RAW 264.7 cells in the presence of different scaffolds. (C) FL microscopy images of hBMSCs cultured under 2D and 3D conditions, showing the expression of the osteogenic markers Runx2 and OCN after 14 days. (D) Histological images of the calvarial defect region showing vascularised bone regeneration. Rats that did not receive scaffold treatment served as the negative Ctrl group, whereas rats treated with GelMA and GelMA-Y scaffolds served as the positive Ctrl and experimental groups, respectively. Black lines indicate the regions of interest. Yellow arrows indicate areas containing osteoblasts. Figure reprinted with permission from Dutta *et al.*[121] Copyright © 2023 Wiley-VCH GmbH.

Abbreviations: 3DP: Three-dimensional printed; ALP: Alkaline phosphatase; BV: Blood vessel; CQDs: Carbon quantum dots; Ctrl: Control; DAPI: 4′,6-Diamidino-2-phenylindole; Dox: Doxorubicin; FL: Fluorescence; FT: Fibrous tissue; G-CQDs: Green carbon quantum dots; GelMA: Gelatin methacryloyl; GelMA-G: Gelatin methacryloyl containing green carbon quantum dots; GelMA-Y: Gelatin methacryloyl containing yellow carbon quantum dots; H&E: Hematoxylin and eosin; hBMSCs: Human bone marrow-derived mesenchymal stem cells; IO: Immature osteocytes; MO: Mature osteocytes; M-CM: Macrophage-conditioned medium; NB: New bone; NIR: Near-infrared; OCN: Osteocalcin; OPN: Osteopontin; PTX: Paclitaxel; Runx2: Runt-related transcription factor 2; Y-CQDs: Yellow carbon quantum dots.

dots have also been incorporated into sonodynamic therapeutic systems that combine antibacterial activity with osteogenic stimulation, further demonstrating the potential of CQDs to integrate stimulus-responsive therapy with bone regeneration.[125] In the context of bioprinting, these functionalities could support the development of active bioinks with spatially controlled photoresponsiveness, drug delivery, or anti-infective activity. Direct experimental evidence for such applications, however, remains limited.

Compared with GO, CQDs are more analogous to functional nanocarriers, with their major advantages arising from their small size, surface tunability, and optical and delivery capabilities rather than from directly improving the macroscopic mechanical properties of bioinks. Currently, direct experimental evidence supporting CQD-enhanced bone bioinks remains relatively limited, and most evidence regarding the osteogenic, antibacterial, and immunomodulatory effects of CQDs is derived from non-printed hydrogel systems or nanodelivery platforms. Therefore, the regenerative effects of CQDs should be primarily attributed to their multifunctional roles in bioactive molecule delivery, surface-mediated cellular regulation, and microenvironmental modulation, rather than simply mechanical reinforcement of bioinks. The

influence of CQDs on osteogenic differentiation may further depend on the synergistic regulation of cell–material interactions, intracellular signalling, and local biochemical cues.

4.4. Two-dimensional nanomaterial-enhanced bioinks

Two-dimensional nanomaterials typically possess atomic- or nanoscale thicknesses combined with comparatively large lateral dimensions, resulting in high specific surface areas and abundant interfacial interaction sites. Their potential extends beyond the mechanical reinforcement traditionally associated with inorganic nanoparticles to include electrical activity, photothermal conversion, surface adsorption, and tunable degradation, making them attractive candidates for bioinks that integrate structural support with active biological regulation.[126] At present, however, the application of 2D nanomaterials in 3D-printed bone tissue engineering remains at a relatively early stage. Studies that simultaneously fulfil the criteria of incorporating a 2D nanomaterial into a cell-laden bioink for bone bioprinting remain limited, with the most direct evidence currently available for MXenes.

MXenes are a family of 2D transition-metal carbides, nitrides, and carbonitrides, among which $Ti_3C_2T_x$ is the most extensively investigated member in biomedical applications. Its surface generally contains abundant hydroxyl, oxygen, and fluorine terminations, which favour aqueous dispersion and confer high electrical conductivity and interfacial activity. Lee *et al.*[17] incorporated $Ti_3C_2T_X$ MXene into a GelMA/HAMA composite hydrogel and directly encapsulated hMSCs for 3D bioprinting. MXene incorporation improved bioink rheology and structural stability while maintaining favourable post-printing cell viability and proliferation. More importantly, even in the absence of conventional osteogenic supplements, MXene-containing constructs exhibited increased ALP activity, mineralisation, and osteogenesis-related marker expression, suggesting that 2D $Ti_3C_2T_X$ can directly modify the hMSC microenvironment and promote spontaneous osteogenic differentiation. The influence of MXene on bioink performance is not restricted to osteogenic regulation. Nelson *et al.*[127] compared the effects of $Ti_3C_2T_X$ MXene and graphene/GO on the physical properties of alginate–cellulose bioinks. MXene incorporation increased the compressive Young's modulus of the printed constructs by approximately 72% and electrical conductivity by 0.39 S/m, whereas graphene/GO predominantly increased conductivity with a comparatively limited effect on compressive modulus. C2C12 cell viability remained above 95% across the different nanomaterial-containing groups. Black phosphorus represents another potentially valuable 2D material for bone bioink development. Black phosphorus nanosheets exhibit high surface reactivity and degrade into phosphorus-containing products, and they have already demonstrated mineralisation-promoting, photothermal, and drug-delivery capabilities in conventional bone tissue-engineering hydrogels and 3D-printed scaffolds. Combined use of black phosphorus with other 2D materials such as GO has also been reported to enhance cell proliferation and osteogenesis.[128] A similar evidence pattern applies to molybdenum disulfide and other transition-metal dichalcogenides. These materials offer large specific surface areas together with photothermal and surface-functionalisation potential and have shown promise in bone defect treatment, hydrogel-based delivery, and tumour-associated bone regeneration. However, direct evidence from cell-laden bone bioprinting remains scarce.

Two-dimensional nanomaterials exhibit unique advantages in bone tissue bioprinting due to their atomic-scale thickness, high specific surface area, and abundant surface-active sites, distinguishing them from conventional nanoparticles. Unlike ceramic nanomaterials that primarily function through mineral composition and ion release, the biological functions of 2D nanomaterials are largely derived from their distinctive physicochemical properties, including surface adsorption, electrical responsiveness, photothermal conversion, and redox regulation. For example, the oxygen-containing functional groups on GO surfaces can enhance interactions between materials and biomolecules and regulate cell–material interfacial behaviours, thereby influencing the osteogenic differentiation of MSCs. Experimental studies have demonstrated that incorporating GO nanosheets into GelMA systems enhances the mineralisation capacity of hMSC-laden constructs and promotes osteogenic responses through BMP–SMAD-related signalling pathways, indicating that the effects of GO are not solely attributed to mechanical reinforcement but also involve its surface chemistry and ability to regulate cellular signalling.[93] In contrast, conductive 2D materials such as MXene primarily provide additional functionalities to bioinks through their excellent electrical conductivity and photothermal conversion properties. For instance, Ti_3C_2 MXene-incorporated hydrogels can achieve antibacterial effects through near-infrared-induced photothermal responses while simultaneously improving osseointegration and bone formation in infected bone defect environments, suggesting that 2D materials can facilitate tissue regeneration through modulation of the local microenvironment rather than relying solely on direct osteogenic stimulation.[129] Therefore, the regenerative effects of 2D nanomaterial-enhanced bioinks should be interpreted in the context of their intrinsic physicochemical characteristics, including

interfacial adsorption, electrical properties, photothermal responsiveness, and cell–material interactions, rather than being simply attributed to increased ALP expression or mineralisation levels.

However, the incorporation of 2D nanomaterials into bioink systems also raises new concerns regarding long-term biosafety. Parameters including lateral size, layer number, surface functional groups, and oxidation state may influence their dispersion stability, cellular uptake, and *in vivo* degradation behaviour. MXene materials may undergo oxidation in aqueous and oxygen-rich environments, resulting in alterations of their structure and functionality. Although black phosphorus exhibits degradable characteristics, the release of phosphorus species and degradation kinetics during degradation may affect the local microenvironment and tissue regeneration process. Previous studies have demonstrated that black phosphorus nanosheets can promote vascularised bone regeneration through sustained phosphorus release and regulation of angiogenesis and osteogenesis, while their degradation behaviour is highly dependent on material design and modification strategies.[130,131] Therefore, future evaluation of 2D nanomaterial-enhanced bioinks should not rely solely on short-term indicators such as ALP activity, osteogenic gene expression, or mineralisation outcomes, but should additionally incorporate nanosheet degradation kinetics, cellular internalisation, immune responses, *in vivo* clearance behaviour, and long-term tissue remodelling effects to comprehensively assess their true regenerative potential and clinical translational value.

4.5. Polymeric and fibrous nanomaterial-enhanced bioinks

Polymeric and fibrous nanomaterials reinforce bioinks through mechanisms distinct from those of inorganic particles and 2D nanosheets. Rather than primarily providing therapeutic ions, these materials generally establish nanoscale fibrous networks that increase polymer-chain entanglement and physical crosslinking, thereby enhancing shear-thinning behaviour, yield characteristics, and post-deposition stability.[119] Nanocellulose represents the most extensively investigated example and includes cellulose nanofibrils (CNFs) and cellulose nanocrystals. Owing to their high aspect ratio, CNFs can form continuous fibrous networks at relatively low concentrations and are therefore frequently combined with alginate, gelatin, and GelMA to compensate for the insufficient viscosity and limited shape retention of hydrogel-only formulations.

Ojansivu *et al.*[132] established an early representative nanocellulose-based system for bone bioprinting by incorporating wood-derived CNFs and bioactive glass into a gelatin/alginate bioink containing Saos-2 cells or BMSCs. CNFs markedly altered hydrogel flow behaviour and improved printability, while the bioactive glass retained its ion-releasing activity. Printed BMSCs exhibited greater tolerance than Saos-2 cells, with favourable cell viability, proliferation, and ALP activity observed during 14 days of culture. Bioactive glass further enhanced early osteogenesis-related responses. This composite strategy was subsequently extended by Lafuente-Merchan *et al.*,[18] who used a nanocellulose/alginate formulation as the base bioink and separately incorporated HA and GO to fabricate bone tissue bioprinting constructs. Both functional additives altered the material properties of the composite bioink while supporting post-printing cell survival and bone-related differentiation. These findings also indicate that CNF content should not be optimised independently of the surrounding formulation, as its effects depend on polymer concentration, crosslinking strategy, and the availability of cell-adhesive sites within the overall composite network. CNFs can be further combined with nHA to create multiscale networks that more closely resemble the hierarchical organisation of bone matrix. In subsequent work, Korkeamäki *et al.*[100] incorporated different concentrations of nHA into GelMA/gelatin/CNF formulations. The rheological support provided by CNFs improved printing stability, while an appropriate nHA content further enhanced osteogenesis-related responses. Excessive mineral loading nevertheless increased viscosity and interfered with photocrosslinking, demonstrating that the relative proportions of the fibrous network and inorganic particles require careful optimisation. Such findings suggest that nanocellulose is more appropriately used as a structural framework for bioink formulation rather than as a standalone osteoinductive component.

The primary advantages of nanocellulose-enhanced bioinks arise from their high aspect ratio, nanoscale fibrous network structure, and physical interactions with polymer chains, rather than from direct induction of osteogenic differentiation. CNFs can form nanoscale reinforcing networks that enhance bioink viscoelasticity, shear-thinning behaviour, and post-printing shape fidelity, thereby improving structural stability during extrusion-based bioprinting.[133] However, these reinforcing effects are strongly concentration-dependent. Insufficient CNF content may fail to establish an adequate network structure, whereas excessive concentrations can increase viscosity and extrusion pressure while restricting cell migration and nutrient diffusion. Therefore, the design of CNF-enhanced bioinks requires an appropriate balance between printability and the cellular microenvironment, rather than simply increasing fibre content to improve material performance. Unlike natural protein-based materials such as collagen

and gelatin, native cellulose lacks the adhesion sequences required for mammalian cell recognition. Consequently, CNFs often require surface functionalisation, such as RGD modification, or incorporation with GelMA, gelatin, and extracellular matrix-derived components to enhance cell adhesion and biological activity.[134,135] Recent studies have further demonstrated that nanocellulose can serve not only as a mechanical reinforcing component but also as a platform for biomolecular delivery and interfacial regulation.[135,136] Its abundant surface hydroxyl groups and modifiable functional groups enable the adsorption or immobilisation of growth factors, proteins, and other bioactive molecules, thereby indirectly regulating cellular behaviour.[135] Accordingly, the regenerative effects of CNF-enhanced bioinks should not be simply attributed to direct osteogenic stimulation, but rather to their regulation of the 3D microenvironment, cell adhesion, and functional component delivery. Furthermore, the long-term *in vivo* degradation and clearance of nanocellulose remain important considerations for its clinical translation. Because mammals lack an effective endogenous cellulase system, unmodified nanocellulose may exhibit slow degradation or prolonged tissue retention. Its degradation behaviour is influenced by several factors, including crystallinity, degree of oxidation, fibre structure, and host immune responses.[136] Therefore, future development of CNF-enhanced bioinks should move beyond simply increasing cellulose content. Instead, CNFs should be utilised to establish stable printable networks while being integrated with HA, bioactive glass, GO, or bioactive molecules to introduce osteoinductive, angiogenic regulatory, and immunomodulatory functions. This approach could improve bioink printability while supporting its regenerative functionality.

5. Long-term biosafety, regulatory challenges, and clinical translation

Despite the demonstrated advantages of nanomaterial-enhanced bioinks in improving printability, osteogenic differentiation, angiogenesis, and immunomodulation *in vitro* and in animal bone defect models, their clinical translation remains substantially limited by concerns regarding long-term biosafety and regulatory uncertainties. A critical issue is that nanomaterials incorporated into bioinks may not remain permanently confined within the hydrogel network after implantation. As hydrogels undergo swelling, enzymatic degradation, cell-mediated matrix remodelling, and long-term mechanical stress, some nanoparticles, nanosheets, or their degradation products may gradually be released into surrounding tissues, subsequently internalised by macrophages, and transported through lymphatic or blood circulation systems, resulting in potential systemic distribution. Therefore, the safety evaluation of nanomaterial-enhanced bioinks should not rely solely on short-term post-printing cell viability or local histological outcomes, but should instead establish a comprehensive evaluation framework covering nanoparticle release, local transformation, tissue distribution, degradation, and eventual clearance.[137] The long-term risks of different nanomaterials should also not be assessed using identical criteria. For inorganic nanomaterials such as nHA, CaP, and bioactive glass, their clinical risks depend not only on whether intact particles migrate from the implantation site but also on material dissolution, phase transformation, and cumulative release of Ca, P, Si, and doped metal ions. Therefore, both particle retention and ion release kinetics should be systematically monitored. In contrast, 2D nanomaterials such as GO and MXene exhibit more complex size-dependent behaviours, surface chemistry, and *in vivo* transformation processes. A study in mice demonstrated that intravenously administered GO with particle sizes below approximately 300 nm can distribute to the liver, spleen, and kidneys, with predominant accumulation in the liver during early stages accompanied by alterations in serum biochemical parameters and oxidative stress indicators.[138] Another study further demonstrated that GO nanosheets with sizes of approximately 70 nm and 300 nm exhibited distinct hepatic clearance behaviours, with smaller GO showing greater hepatobiliary excretion while larger nanosheets exhibited slower clearance, indicating that particle size itself can significantly influence *in vivo* retention and toxicity.[139] Although these intravenous exposure studies cannot be directly equated with the actual exposure levels generated by gradual local release from hydrogels in bone defects, they highlight that even nanomaterials with identical chemical compositions may exhibit completely different biological fates depending on particle size, aggregation state, and surface modification. Therefore, human safety thresholds cannot be simply extrapolated from a single non-toxic concentration determined *in vitro*. For MXene materials, oxidation and surface chemical changes may occur under aqueous and oxygen-containing conditions, which not only compromise their original electrical and material properties but may also alter degradation products and cellular exposure patterns.[140] Systemic exposure studies of Ti_3C_2 nanosheets have demonstrated their distribution in the lungs and liver, and prolonged exposure was associated with alterations in pulmonary physiological functions, further indicating that the absence of obvious short-term histopathological changes does not necessarily guarantee long-term biosafety.[141] Therefore, the oxidation degree and lateral dimensions of GO, the surface termination groups and oxidation state of MXene, as well as the dynamic changes of these properties during

Table 1. Comparative summary of representative nanomaterial-enhanced bioinks and related printed scaffolds for bone regeneration

Nanomaterial (type/size)	Concentration and bioink composition	Printing method and key parameters	Cell type and incorporation method	Post-print cell viability	Biological evidence (*in vitro*/*in vivo*)	Major limitations	Reference
nHA; size NR	GelMA/gelatin/CNF; nHA 0, 1, 3, 5% w/v	Extrusion + photocuring; 1% improved shape fidelity; other parameters NR	hBMSCs; Enc	High at 1% nHA; lower at 5%; quantitative %/time NR	*In vitro*: 1% nHA supported Runx2, type I collagen, dentin matrix protein 1, OCN; 5% hindered curing and cell performance. *In vivo*: Not evaluated.	Narrow dose window; excessive nHA impaired photocrosslinking and structural stability.	100
Mg-doped nHA (needle-like and rounded); size NR	Gelatin 5% + GelMA 5% + nHA 1% w/w	Extrusion; 0.51-mm needle; 27° C; ~0.5 bar, 11.3 mm/s	hBMSCs; Enc	High (Live/Dead, days 1, 7, 14, and 21); quantitative % NR	*In vitro*: chemistry/morphology affected metabolic activity and Runx2, ALP, OCN expression over 21 d. *In vivo*: Not evaluated.	Single nanoparticle dose; shape, crystallinity and composition vary concurrently.	19
nHA; size NR	dECM 2 g + gelatin 5 g + QCS 1 g/100 mL; nHA 0–5.3 g/100 mL; Exo after printing	Extrusion; 0.31-mm needle; 0.24–0.27 MPa; 8–10 mm/s	Ac; hADSC Exo loaded afterwards; HUVEC assays	Not applicable (no cells Enc during printing)	*In vitro*: antibacterial activity, cell attachment and angiogenic/osteogenic responses. *In vivo*: rat, 6-mm calvarial defect, 10 wk; improved new bone. Mouse Matrigel angiogenesis assay: 1 wk.	Exosome-loaded acellular scaffold, not a cell-laden bioink; contributions of nHA/QCS/Exo coupled.	101
CaP (<150 nm) or GO (~10 nm)	GelMA 100 mg/mL + LAP 5 mg/mL; CaP 50 mg/mL (+ BB 0.5 mg/mL) or GO 0.5 mg/mL	DLP; 100-μm layer; 37 °C; 9-s exposure; ~33.6 mW/cm^2	hMSCs; Enc	Qualitative Live/Dead at d7 and d14; % NR (CaP showed more dead cells)	*In vitro*: CaP increased osteogenic genes and calcium deposition; GO mainly increased modulus/altered cell morphology. *In vivo*: Not evaluated.	Unequal CaP/GO doses; donor variation; no animal validation.	11
Nano-β-TCP; size NR	Outer GelMA/alginate + 0–3% nano-β-TCP; middle GelMA/alginate; sacrificial gelatin core	Triaxial bioprinting; distinct osteogenic/vascular layers	MC3T3-E1 (outer) + HUVECs (middle); Enc	> 90% (d7; across tested formulations)	*In vitro*: 3% β-TCP produced higher ALP, OCN, and CD31. *In vivo*: Not evaluated.	*In vitro* vascularised-bone model only; multilayer flow coordination.	68
Citrate- or acetate-stabilised ACP; size NR	ACP_CIT or ACP_ACE + ADA-GEL	Extrusion, 65 kPa, 5 mm/s; CaCl2 and microbial TGase post-crosslinking	MC3T3-E1; Enc	Cytocompatible by microscopy; numerical %/measurement time NR	In vitro: ACP_CIT improved construct shape stability; cell staining confirmed cytocompatibility. In vivo: Not evaluated.	Limited direct osteogenic outcomes and dose/size characterisation.	106

(*Cont'd...*)

Table 1. (*Continued*)

Nanomaterial (type/size)	Concentration and bioink composition	Printing method and key parameters	Cell type and incorporation method	Post-print cell viability	Biological evidence (*in vitro*/*in vivo*)	Major limitations	Reference
nHA; size NR	GelMA/gelatin/CNF; nHA 0, 1, 3, 5% w/v	Extrusion + photocuring; 1% improved shape fidelity; other parameters NR	hBMSCs; Enc	High at 1% nHA; lower at 5%; quantitative %/time NR	*In vitro*: 1% nHA supported Runx2, type I collagen, dentin matrix protein 1, OCN; 5% hindered curing and cell performance. *In vivo*: Not evaluated.	Narrow dose window; excessive nHA impaired photocrosslinking and structural stability.	100
Aminated Cu-MBGNs; size NR	ACuMBGNs + alginate dialdehyde/gelatin (ADA-GEL); particle dose NR	Extrusion; reversible covalent/enzymatic/ ionic network; good shape retention	Human osteosarcoma cells, ST2 mouse stromal cells; Enc; primary mouse BMSCs tested	>90% viable (reported; day-specific % NR); rapid spreading by d3	*In vitro*: BMSC osteogenesis and angiogenesis promoted without added growth factors. *In vivo*: Not evaluated.	Glass-ion and dynamic-network contributions not separated.	9
Laponite nSi (1–2 nm thick; 20–50 nm wide)	NICE: GelMA 7.5% + κ-carrageenan 1% + nSi 2% + Irgacure 2959 0.25%	Screw extrusion; ~37 °C; 365-nm photocuring for 60 s	hMSCs; Enc	Viable over long-term culture (to 60 d); quantitative % NR	*In vitro*: cell-driven matrix remodelling and endochondral osteogenic differentiation/ mineralization. *In vivo*: Not evaluated.	No orthotopic bone-defect validation; high polymer/ nSi load may affect extrusion.	14
Laponite nanosilicate; size NR	Gelatin 10% + alginate 1% + nSi 0–3% (optimal 2%)	Extrusion; 22G; 50 mm/s; 2% $CaCl_2$ ×10 min	Rat BMSCs; Enc	Live/Dead at d1, 3, 5, 7, 14, 21; quantitative % NR	*In vitro*: enhanced osteogenic markers/mineralization. *In vivo*: rat, 8-mm calvarial defect; 2, 4, 8, 12 wk; faster bridging and bone formation.	Non-load-bearing small animal site; long-term nanosilicate clearance unknown.	15
CS nanowires (10–50 nm diameter)	GelMA + CS nanowires; particle dose NR	Bilayer multicellular extrusion; neural upper/osseous lower layer	Schwann cells + BMSCs; Enc in distinct layers	Long-term cell survival reported; %/ time NR	*In vitro*: neurogenic and osteogenic responses increased. *In vivo*: rat critical-sized calvarial defect; 4 and 8 wk; enhanced nerve ingrowth and bone formation.	Multicellular design limits attribution to one nanomaterial effect.	114
Sr-substituted CSH (xonotlite) nanowires; size NR	GelMA 10% + Sr-CSH 5%	Extrusion; printing speed/pressure NR	BMSCs; Enc; macrophages studied separately	Biocompatible; quantitative post-print %/time NR	*In vitro*: BMSC osteogenesis and M2-associated macrophage response. *In vivo*: rat critical-sized calvarial defect; follow-up NR; enhanced bone regeneration.	Small-animal site; effects of Sr, Si and Ca ions not fully disentangled.	33

(*Cont'd...*)

Table 1. (*Continued*)

Nanomaterial (type/size)	Concentration and bioink composition	Printing method and key parameters	Cell type and incorporation method	Post-print cell viability	Biological evidence (*in vitro*/*in vivo*)	Major limitations	Reference
Laponite nanoclay; size NR	3% Laponite + 3% alginate + 3% methylcellulose (3-3-3)	Extrusion; ~410-μm nozzle; 100 mM $CaCl_2$ ×10 min	hBMSCs: Enc; HUVECs: Seed after printing (CAM arm); BMP-2: Ac	hBMSCs viable over 21 d; numeric % NR; seeded HUVEC post-print viability N/A	*In vitro*: osteogenic mineralisation; *ex vivo*: chick CAM, 7 d, vessel ingrowth. *In vivo*: mouse subcutaneous ectopic site; BMP-2 arm 4 wk; hBMSC arm followed 2–8 wk.	Different cell/drug-loading arms; ectopic rather than bone-defect model.	43
Rod-like nano-ATP; size NR	nano-ATP/GelMA; graded ATP doses	Extrusion, photo-crosslinking; pressure/speed NR	Mouse BMSCs + MUVECs (*in vitro*), rat BMSCs (implant arm); Enc	High post-print viability reported; percentage/time NR	*In vitro*: BMSC osteogenesis and endothelial angiogenesis. *In vivo*: rat calvarial defect; follow-up NR; enhanced bone and vessel formation.	Different cell sources; nanoparticle dose/ long-term mechanics incompletely described.	10
Sr-doped nano-ATP (parent 150–500 nm)	Sr-ATP/GelMA/ chitosan Pickering emulsion; Sr-ATP 0%–2%	Emulsion-templated 3D extrusion printing; printing parameters NR	BMSCs in subsequent assays; inclusion during printing not confirmed (NR)	Post-print viability NR (cannot equate later seeded-cell viability with bioprinting viability)	*In vitro*: improved BMSC proliferation/osteogenic markers and endothelial tube formation. *In vivo*: rat cranial defect; follow-up NR; improved osteogenesis/angiogenesis.	Direct cell incorporation during printing not substantiated by accessible methods.	117
GO nanosheets; size NR	Alginate/gelatin + GO 0.5, 1, 2 mg/mL	Extrusion; GO improved fidelity; detailed pressure/ speed NR	hMSCs; Enc	Live/Dead evaluated d1, d7, d42; exact % NR; viability higher at d1 with GO	*In vitro*: 1 mg/mL increased *ALPL*, *BGLAP*, *PHEX*; highest mineral volume at d42. *In vivo*: Not evaluated (mouse calvarial geometry was an *in vitro* printed model).	High GO dose led to swelling and reduced long-term modulus.	16

(*Cont'd...*)

Table 1. (*Continued*)

Nanomaterial (type/size)	Concentration and bioink composition	Printing method and key parameters	Cell type and incorporation method	Post-print cell viability	Biological evidence (*in vitro*/*in vivo*)	Major limitations	Reference
Polyphenol CQDs (few-nm scale; exact size NR)	GelMA 12 wt% + CQDs 100 μg/mL; photoactivated delivery	Extrusion; ~65 kPa; 365-nm curing; 808-nm NIR (1 W/cm^2)	hBMSCs; Enc; RAW264.7 macrophages and osteosarcoma cells assayed	Quantitative post-print viability/time NR; bioprinted hBMSCs formed vessel-like structures by d14	*In vitro*: macrophage M2-associated response, osteogenesis, angiogenesis-like structures, and NIR-triggered antitumor activity. *In vivo*: Rat calvarial defect model; the printed GelMA-Y scaffolds promoted new bone formation and vascularised bone regeneration, with follow-up assessments at 2 and 8 weeks.	Predominantly *in vitro* platform; no demonstrated animal bone-defect repair.	121
$Ti_3C_2T_x$ MXene nanosheets; size NR	GelMA/HAMA (400:1) + MXene 50 μg/mL + Irgacure 2959 0.1%	BioX extrusion; 580-μm nozzle; 20 kPa; 6 mm/s; bed/nozzle 15 °C	hMSCs; Enc	Live/Dead at d1, d3, d5; numerical cell viability % NR	*In vitro*: spontaneous ALP elevation, osteogenic gene expression and mineralisation without supplements. *In vivo*: Not evaluated.	Dose-dependent MXene cytotoxicity at higher concentrations; no long-term animal data.	17
Wood-derived CNF + BaG; size NR	CNF ~0.25% + alginate 4% + gelatin 5% + BaG 1%	3D-Bioplotter extrusion; ~1.5–3.2 bar, 17–65 mm/s; $CaCl_2$ 100 mM	Saos-2 cells and hBMSCs (separate groups); Enc	Viability assessed during 14-d culture; quantitative % NR; hBMSCs tolerated extrusion better	*In vitro*: cell viability/ALP responses; BaG stimulated early BMSC osteogenic commitment, but reduced Saos-2 viability. *In vivo*: Not evaluated.	Strong cell-type effects and BaG-associated viscosity changes.	132

Abbreviations: β-TCP: Beta-tricalcium phosphate; Ac: Acellular; ACP: Amorphous calcium phosphate; ACP_ACE: Acetate-stabilized amorphous calcium phosphate; ACP_CIT: Citrate-stabilized amorphous calcium phosphate; ACuMBGNs: Amine-functionalized copper-doped mesoporous bioactive glass nanoparticles; ADA-GEL: Alginate dialdehyde–gelatin; ALP: Alkaline phosphatase; ATP: Attapulgite; BaG: Bioactive glass; BB: Brilliant Black; BMP-2: Bone morphogenetic protein 2; BMSCs: Bone marrow-derived mesenchymal stem cells; CAM: Chorioallantoic membrane; CaP: Calcium phosphate; CNF: Cellulose nanofibrils; CQDs: Carbon quantum dots; CS: Calcium silicate; CSH: Calcium silicate hydrate; dECM: Decellularised extracellular matrix; DLP: Digital light processing; Enc: Encapsulated; Exo: Exosomes; GelMA: Gelatin methacryloyl; GO: Graphene oxide; HAMA: Hyaluronic acid methacrylate; hADSCs: Human adipose-derived stem cells; hBMSCs: Human bone marrow-derived mesenchymal stem cells; hMSCs: Human mesenchymal stem cells; HUVECs: Human umbilical vein endothelial cells; LAP: Lithium phenyl-2,4,6-trimethylbenzoylphosphinate; MUVECs: Mouse umbilical vein endothelial cells; N/A: Not applicable; nHA: Nanohydroxyapatite; NICE: Nanoengineered ionic-covalent entanglement; NIR: Near-infrared; NR: Not reported; nSi: Nanosilicate; OCN: Osteocalcin; QCS: Quaternized chitosan; Runx2: Runt-related transcription factor 2; Sr-CSH: Strontium-substituted calcium silicate hydrate; TGase: Transglutaminase.

doi: 10.36922/IJB026350383

storage, printing, sterilisation, and implantation, should be considered critical parameters in biosafety evaluation.

The biosafety of nanomaterials is also strongly dependent on dosage and exposure duration. Appropriate amounts of nanoparticles may improve bioink rheological properties, mechanical performance, and osteogenic activity, whereas further increases in concentration may induce particle aggregation, enhanced cellular uptake, oxidative stress, membrane damage, or persistent immune activation. Indeed, previous studies discussed in this review have revealed similar optimal concentration windows. Higher nHA contents may increase viscosity and interfere with photopolymerisation, thereby reducing cell viability and osteogenic performance. Likewise, increasing GO concentration does not necessarily result in a linear enhancement of osteogenesis, as nanosheet concentration, size, oxidation degree, and surface functional groups can substantially alter cellular responses. Therefore, future studies should transform the currently used material concentration ranges for optimising printing performance into clinically meaningful therapeutic–safety windows. Beyond conventional assessments of cell viability and osteogenic markers, comprehensive evaluation should include long-term macrophage activation, pro-inflammatory cytokine secretion, oxidative stress, genotoxicity, degradation products, as well as nanoparticle accumulation and tissue responses in major organs such as the liver, spleen, kidney, and lung. Furthermore, observation periods should be extended until substantial material degradation or stable tissue integration has been achieved. Even for materials generally considered highly biocompatible, such as nanocellulose, potential differences arising from raw material sources, residual impurities, and manufacturing processes must be carefully considered, as natural origin does not necessarily guarantee long-term biosafety.[142]

In addition to toxicological concerns, batch-to-batch consistency, sterilisation, manufacturing scalability, and quality control present substantial challenges to the regulatory approval of nanomaterial-enhanced bioinks. Bioprinted products simultaneously involve cells, hydrogels, nanomaterials, and specific manufacturing processes; therefore, depending on their composition, primary mechanism of action, and intended application, they may fall under different regulatory frameworks, including medical devices, biological products, tissue-engineered products, or combination products. Currently, fully harmonised regulatory pathways for bioprinting products have not yet been established across different regions.[143-145] The incorporation of nanomaterials further increases quality control complexity. For example, variations may occur among different batches of GO in lateral size and oxidation degree, among MXene materials in surface termination groups and oxidation states, among nHA particles in crystallinity and particle size, and among naturally derived nanocellulose materials in impurity composition. Therefore, during clinical translation, clearly defined critical quality attributes should be established, including particle size and distribution, morphology, surface charge, chemical composition, oxidation state, purity, endotoxin levels, dispersion stability, ion or particle release kinetics, as well as the rheological properties, crosslinking behaviour, cell viability, and printing fidelity of the final bioink.[146] Sterilisation represents another major challenge distinguishing cell-laden bioinks from conventional implant materials. Since final products containing living cells are generally incompatible with conventional terminal sterilisation methods, non-cellular components require validated sterilisation procedures, followed by cell incorporation, mixing, and printing under sterile or controlled conditions. Meanwhile, it is essential to verify whether sterilisation alters polymer molecular structures, nanomaterial surface chemistry, particle aggregation behaviour, rheological properties, or final cytocompatibility. As manufacturing scales increase from laboratory millilitre volumes to clinically relevant dimensions, issues related to mixing efficiency, particle sedimentation, cell distribution, printing platform variability, and batch reproducibility may become further amplified. Therefore, raw material standardisation, manufacturing processes compliant with Good Manufacturing Practice, clearly defined process controls, and validated product release criteria are essential for achieving scalable and reproducible production.

Another important translational limitation originates from the selection of current *in vivo* models. A large proportion of existing studies on nanomaterial-enhanced bone bioprinting rely on mouse or rat critical-sized calvarial defect models. Although these models are useful for rapidly evaluating osteogenic capacity and material compatibility, the calvarium represents a relatively non-load-bearing site, and its defect size, mechanical loading conditions, bone remodelling pattern, and host immune environment cannot fully replicate large load-bearing long bone defects in humans. Previous studies have also demonstrated substantial variations in the definition of critical-sized defects among different animal species, ages, anatomical locations, and defect dimensions, and a fully standardised methodology has not yet been established.[147] Therefore, directly extrapolating increased new bone area or BV/TV values obtained from small animal calvarial models to clinical outcomes in large load-bearing bone defects should be interpreted with caution. Future studies

should progressively move towards larger animal models, including rabbits, sheep, goats, pigs, or dogs, and employ segmental long bone defects or other load-bearing defect models to evaluate construct stability and osseointegration under physiological mechanical loading conditions.[147,148] Evaluation endpoints should also be expanded beyond micro-computed tomography and histological assessment of new bone formation to include long-term material degradation, systemic nanomaterial distribution, chronic immune responses, vascularisation, infection risk, as well as functional parameters such as compressive, bending, torsional, and fatigue performance. Only when nanomaterial-enhanced bioinks demonstrate reproducible bone regeneration, functional restoration, and acceptable local and systemic safety under larger-scale, long-term, and load-bearing conditions can they truly progress from experimental material platforms towards clinically applicable bone regenerative products.

6. Future perspectives

Nanomaterial-enhanced bioinks have substantially expanded the functional scope of bone tissue bioprinting by enabling simultaneous regulation of printing behaviour, structural stability, and regenerative bioactivity. Rather than acting simply as reinforcing fillers, nanomaterials can interact with polymer networks, cells, proteins, and the surrounding ionic environment to reshape the physicochemical and biological properties of printed constructs. Ceramic nanomaterials such as nHA and other CaP phases primarily provide bone-mimetic mineral environments and support osteogenic differentiation and mineralisation, while BGNs introduce composition-dependent ion release and additional opportunities for multifunctional regulation. Nanosilicates and nanoclays combine rheological reinforcement with ion-mediated signalling and molecular adsorption, allowing bioinks to regulate osteogenesis, vascularisation, innervation, and immune responses. Carbon-based and 2D nanomaterials provide distinct interfacial, electrical, optical, and surface-functionalisation properties, whereas nanocellulose and related fibrous nanomaterials can establish continuous nanoscale networks that improve shear-thinning behaviour and post-printing structural stability. Collectively, these studies demonstrate that the value of nanomaterials lies not in maximising a single property, but in coordinating printability, cellular compatibility, mechanical behaviour, and regenerative function within the same bioink. The increasing use of multicellular printing, spatially separated mineral and vascular compartments, self-mineralising constructs, and immunomodulatory systems further indicates that bone bioprinting is progressing from the fabrication of cell-laden hydrogel scaffolds towards the reconstruction of more integrated regenerative microenvironments.

Several challenges nevertheless limit the translation of nanomaterial-enhanced bioinks into reproducible and clinically relevant bone regeneration strategies. Nanomaterial concentration, particle size, morphology, crystallinity, surface chemistry, oxidation state, and dispersion can markedly alter rheology, light propagation, crosslinking, degradation, ion release, cellular uptake, and tissue responses, making comparisons between studies difficult and preventing simple relationships between nanomaterial content and biological performance. Future studies should therefore establish quantitative formulation windows that link nanomaterial characteristics with printability, structural fidelity, cellular viability, osteogenic activity, and long-term matrix remodelling rather than relying primarily on comparisons between formulations with and without nanoparticles. Particular attention should also be given to the dynamic requirements of bone repair. An ideal bioink should support early cell survival and appropriate immune responses, facilitate subsequent vascular invasion and osteogenic differentiation, and ultimately permit progressive replacement of the artificial matrix by mature bone tissue. This will require greater control over nanomaterial degradation, ion and molecular release kinetics, spatial distribution, and interactions with macrophages, endothelial cells, skeletal progenitors, osteoblasts, and osteoclasts. More rigorous long-term *in vivo* evaluation is also needed to determine nanomaterial persistence, systemic clearance, degradation products, and their effects on bone remodelling. By integrating nanomaterial engineering with bioink chemistry, advanced printing strategies, multicellular organisation, and biologically informed evaluation, future bone bioprinting systems may evolve from mechanically printable composites into adaptive regenerative platforms capable of coordinating osteogenesis, angiogenesis, immunomodulation, and tissue remodelling throughout the bone healing process.

7. Conclusion

In conclusion, nanomaterial-enhanced bioinks provide a promising approach to overcoming the limitations of conventional bioinks in bone tissue bioprinting by integrating improved printability, mechanical stability, and biological functionality. Different nanomaterial classes contribute through distinct mechanisms, including mineralisation, ion-mediated signalling, interfacial interactions, electrical and optical regulation, and modulation of osteogenic, angiogenic, and immune responses. However, their regenerative performance is highly dependent on material composition, particle

characteristics, concentration, dispersion, and interactions with the polymer network, highlighting that simply increasing nanomaterial content does not necessarily improve biological outcomes. Future advances will require mechanism-guided material selection, coordinated optimisation of bioink formulations and printing parameters, and more rigorous evaluation of long-term biosafety and functional bone regeneration in clinically relevant load-bearing models. Ultimately, integrating nanomaterial engineering with advanced bioprinting and biological microenvironment regulation may facilitate the development of safe, reproducible, and functionally effective constructs for the repair of complex bone defects.

Acknowledgments

None.

Funding

This study received no external funding.

Conflict of interest

The authors declare they have no competing interests.

Author contributions

Conceptualization: Jinbo Zhang
Investigation: Wentao Hu
Supervision: Dedong Liu
Writing–original draft: Yuqiang Wang
Writing–review & editing: Yuqiang Wang, Zhuoxuan Li

Ethics approval and consent to participate

Not applicable.

Consent for publication

Not applicable.

Availability of data

Not applicable.

References

1. de Carvalho ABG, Rahimnejad M, Oliveira R, *et al*. Personalized bioceramic grafts for craniomaxillofacial bone regeneration. *Int J Oral Sci*. 2024;16(1):62.

   doi: 10.1038/s41368-024-00327-7

2. Lei C, Song J-h, Li S, *et al*. Advances in materials-based therapeutic strategies against osteoporosis. *Biomaterials*. 2023;296:122066.

   doi: 10.1016/j.biomaterials.2023.122066

3. Migliorini F, La Padula G, Torsiello E, Spiezia F, Oliva F, Maffulli N. Strategies for large bone defect reconstruction after trauma, infections or tumour excision: a comprehensive review of the literature. *Eur J Med Res*. 2021;26(1):118.

   doi: 10.1186/s40001-021-00593-9

4. Chen S, Wang M. Fabrication, Properties, and Applications of Scaffolds for Bone Tissue Regeneration. *Adv Mater Technol*. 2026;11(9):e01877.

   doi: 10.1002/admt.202501877

5. Xie M, Shi Y, Zhang C, *et al*. In situ 3D bioprinting with bioconcrete bioink. *Nat Commun*. 2022;13(1):3597.

   doi: 10.1038/s41467-022-30997-y

6. Qin Y, Jing Z, Zou D, *et al*. A metamaterial scaffold beyond modulus limits: enhanced osteogenesis and angiogenesis of critical bone defects. *Nat Commun*. 2025;16(1):2180.

   doi: 10.1038/s41467-025-57609-9

7. Liu D, Liu J, Zhao P, *et al*. 3D Bioprinted Tissue-Engineered Bone with Enhanced Mechanical Strength and Bioactivities: Accelerating Bone Defect Repair through Sequential Immunomodulatory Properties. *Adv Healthc Mater*. 2024;13(30):e2401919.

   doi: 10.1002/adhm.202401919

8. Wang J, Wu Y, Li G, *et al*. Engineering Large-Scale Self-Mineralizing Bone Organoids with Bone Matrix-Inspired Hydroxyapatite Hybrid Bioinks. *Adv Mater*. 2024;36(30):e2309875.

   doi: 10.1002/adma.202309875

9. Zhu H, Monavari M, Zheng K, *et al*. 3D Bioprinting of Multifunctional Dynamic Nanocomposite Bioinks Incorporating Cu-Doped Mesoporous Bioactive Glass Nanoparticles for Bone Tissue Engineering. *Small*. 2022;18(12):e2104996.

   doi: 10.1002/smll.202104996

10. Liu C, Dai T, Wu X, *et al*. 3D bioprinting of cell-laden nano-attapulgite/gelatin methacrylate composite hydrogel scaffolds for bone tissue repair. *J Mater Sci Technol*. 2023;135:111-125.

    doi: 10.1016/j.jmst.2022.07.011

11. Kühl J, Krümpelmann SM, Hildebrandt L, *et al*. Nanomaterial-modified bioinks for DLP-based bioprinting of bone constructs: Impact on mechanical properties and mesenchymal stem cell function. *Int J Bioprinting*. 2024;10(6):4015.

    doi: 10.36922/ijb.4015

12. Davern JW, Hipwood L, Bray LJ, Meinert C, Klein TJ. Addition of Laponite to gelatin methacryloyl bioinks improves the rheological properties and printability to create mechanically tailorable cell culture matrices. *APL Bioeng*. 2024;8(1):016101.

    doi: 10.1063/5.0166206

13. Tavares MT, Gaspar VM, Monteiro MV, Farinha JPS, Baleizão C, Mano JF. GelMA/bioactive silica nanocomposite bioinks for stem cell osteogenic differentiation. *Biofabrication*. 2021;13(3):035012

doi: 10.1088/1758-5090/abdc86

14. Chimene D, Miller L, Cross LM, Jaiswal MK, Singh I, Gaharwar AK. Nanoengineered Osteoinductive Bioink for 3D Bioprinting Bone Tissue. *ACS Appl Mater Interfaces*. 2020;12(14):15976-15988.

doi: 10.1021/acsami.9b19037

15. Liu B, Li J, Lei X, *et al*. 3D-bioprinted functional and biomimetic hydrogel scaffolds incorporated with nanosilicates to promote bone healing in rat calvarial defect model. *Mater Sci Eng C Mater Biol Appl*. 2020;112:110905.

doi: 10.1016/j.msec.2020.110905

16. Zhang J, Eyisoylu H, Qin XH, Rubert M, Muller R. 3D bioprinting of graphene oxide-incorporated cell-laden bone mimicking scaffolds for promoting scaffold fidelity, osteogenic differentiation and mineralization. *Acta Biomater*. 2021;121:637-652.

doi: 10.1016/j.actbio.2020.12.026

17. Lee SH, Kang MS, Jeon S, *et al*. 3D bioprinting of human mesenchymal stem cells-laden hydrogels incorporating MXene for spontaneous osteodifferentiation. *Heliyon*. 2023;9(3):e14490.

doi: 10.1016/j.heliyon.2023.e14490

18. Lafuente-Merchan M, Ruiz-Alonso S, Garcia-Villen F, *et al*. 3D Bioprinted Hydroxyapatite or Graphene Oxide Containing Nanocellulose-Based Scaffolds for Bone Regeneration. *Macromol Biosci*. 2022;22(11):e2200236.

doi: 10.1002/mabi.202200236

19. Montanari M, Korkeamaki JT, Campodoni E, *et al*. Effects of Magnesium-Doped Hydroxyapatite Nanoparticles on Bioink Formulation for Bone Tissue Engineering. *ACS Appl Bio Mater*. 2025;8(1):535-547.

doi: 10.1021/acsabm.4c01418

20. Chakraborty A, Roy A, Ravi SP, Paul A. Exploiting the role of nanoparticles for use in hydrogel-based bioprinting applications: concept, design, and recent advances. *Biomater Sci*. 2021;9(19):6337-6354.

doi: 10.1039/d1bm00605c

21. Cai Y, Chang SY, Gan SW, Ma S, Lu WF, Yen CC. Nanocomposite bioinks for 3D bioprinting. *Acta Biomater*. 2022;151:45-69.

doi: 10.1016/j.actbio.2022.08.014

22. Hull SM, Brunel LG, Heilshorn SC. 3D Bioprinting of Cell-Laden Hydrogels for Improved Biological Functionality. *Adv Mater*. 2022;34(2):e2103691.

doi: 10.1002/adma.202103691

23. Li N, Guo R, Zhang ZJ. Bioink Formulations for Bone Tissue Regeneration. *Front Bioeng Biotechnol*. 2021;9:630488.

doi: 10.3389/fbioe.2021.630488

24. Dang Y, Zhang Y, Luo G, *et al*. The decisive early phase of biomaterial-induced bone regeneration. *Appl Mater Today*. 2024;38:102236.

doi: 10.1016/j.apmt.2024.102236

25. Xu G, Chen J, Xiao Z, Xu J, Zhang L, Tang P. Bioaugmented osteosynthesis: precise monitoring and intervention of the bone healing microenvironment. *Bone Res*. 2025;13(1):95.

doi: 10.1038/s41413-025-00466-5

26. Molitoris KH, Huang M, Baht GS. Osteoimmunology of Fracture Healing. *Curr Osteoporos Rep*. 2024;22(3):330-339.

doi: 10.1007/s11914-024-00869-z

27. Newman H, Shih YV, Varghese S. Resolution of inflammation in bone regeneration: From understandings to therapeutic applications. *Biomaterials*. 2021;277:121114.

doi: 10.1016/j.biomaterials.2021.121114

28. Li C, Guo C, Fitzpatrick V, *et al*. Design of biodegradable, implantable devices towards clinical translation. *Nat Rev Mater*. 2019;5(1):61-81.

doi: 10.1038/s41578-019-0150-z

29. Burgan J, Rahmati M, Lee M, Saiz AM. Innate immune response to bone fracture healing. *Bone*. 2025;190:117327.

doi: 10.1016/j.bone.2024.117327

30. Yang L, Shi F, Cao F, *et al*. Neutrophils in Tissue Injury and Repair: Molecular Mechanisms and Therapeutic Targets. *MedComm (2020)*. 2025;6(5):e70184.

doi: 10.1002/mco2.70184

31. Hachemi Y, Perrin S, Ethel M, *et al*. Multimodal analyses of immune cells during bone repair identify macrophages as a therapeutic target in musculoskeletal trauma. *Bone Res*. 2024;12(1):56.

doi: 10.1038/s41413-024-00347-3

32. Zou NY, Liu R, Huang M, *et al*. Age-related secretion of grancalcin by macrophages induces skeletal stem/progenitor cell senescence during fracture healing. *Bone Res*. 2024;12(1):6.

doi: 10.1038/s41413-023-00309-1

33. Yu X, Jiang S, Li D, Shen SGF, Wang X, Lin K. Osteoimmunomodulatory bioinks for 3D bioprinting achieve complete regeneration of critical-sized bone defects. *Composites Part B: Engineering*. 2024;273:111256.

doi: 10.1016/j.compositesb.2024.111256

34. Dutta SD, Ganguly K, Patil TV, Randhawa A, Lim KT. Unraveling the potential of 3D bioprinted immunomodulatory materials for regulating macrophage

polarization: State-of-the-art in bone and associated tissue regeneration. *Bioact Mater*. 2023;28:284-310.

doi: 10.1016/j.bioactmat.2023.05.014

35. Xu Z, Qi X, Bao M, *et al*. Biomineralization inspired 3D printed bioactive glass nanocomposite scaffolds orchestrate diabetic bone regeneration by remodeling micromilieu. *Bioact Mater*. 2023;25:239-255.

doi: 10.1016/j.bioactmat.2023.01.024

36. Kuwahara ST, Liu S, Chareunsouk A, Serowoky M, Mariani FV. On the horizon: Hedgehog signaling to heal broken bones. *Bone Res*. 2022;10(1):13.

doi: 10.1038/s41413-021-00184-8

37. Jeffery EC, Mann TLA, Pool JA, Zhao Z, Morrison SJ. Bone marrow and periosteal skeletal stem/progenitor cells make distinct contributions to bone maintenance and repair. *Cell Stem Cell*. 2022;29(11):1547-1561 e6.

doi: 10.1016/j.stem.2022.10.002

38. Liu YL, Tang XT, Shu HS, Zou W, Zhou BO. Fibrous periosteum repairs bone fracture and maintains the healed bone throughout mouse adulthood. *Dev Cell*. 2024;59(9):1192-1209 e6.

doi: 10.1016/j.devcel.2024.03.019

39. Julien A, Kanagalingam A, Martinez-Sarra E, *et al*. Direct contribution of skeletal muscle mesenchymal progenitors to bone repair. *Nat Commun*. 2021;12(1):2860.

doi: 10.1038/s41467-021-22842-5

40. Sivaraj KK, Majev PG, Jeong HW, *et al*. Mesenchymal stromal cell-derived septoclasts resorb cartilage during developmental ossification and fracture healing. *Nat Commun*. 2022;13(1):571.

doi: 10.1038/s41467-022-28142-w

41. Bixel MG, Sivaraj KK, Timmen M, *et al*. Angiogenesis is uncoupled from osteogenesis during calvarial bone regeneration. *Nat Commun*. 2024;15(1):4575.

doi: 10.1038/s41467-024-48579-5

42. Zhai X, Ruan C, Ma Y, *et al*. 3D-Bioprinted Osteoblast-Laden Nanocomposite Hydrogel Constructs with Induced Microenvironments Promote Cell Viability, Differentiation, and Osteogenesis both In Vitro and In Vivo. *Adv Sci (Weinh)*. 2018;5(3):1700550.

doi: 10.1002/advs.201700550

43. Cidonio G, Glinka M, Kim Y-H, *et al*. Nanoclay-based 3D printed scaffolds promote vascular ingrowth ex vivo and generate bone mineral tissue in vitro and in vivo. *Biofabrication*. 2020;12(3):035010.

doi: 10.1088/1758-5090/ab8753

44. Kim YH, Kanczler JM, Lanham S, *et al*. Biofabrication of nanocomposite-based scaffolds containing human bone extracellular matrix for the differentiation of skeletal stem and progenitor cells. *Biodes Manuf*. 2024;7(2):121-136.

doi: 10.1007/s42242-023-00265-z

45. Del Toro Runzer C, Balmayor ER, van Griensven M. Biologics for bone regeneration: advances in cell, protein, gene, and mRNA therapies. *Bone Res*. 2026;14(1):5.

doi: 10.1038/s41413-025-00487-0

46. Ma Q, Liang M, Wu Y, *et al*. Osteoclast-derived apoptotic bodies couple bone resorption and formation in bone remodeling. *Bone Res*. 2021;9(1):5.

doi: 10.1038/s41413-020-00121-1

47. Sims NA. Osteoclast-derived coupling factors: origins and state-of-play Louis V Avioli lecture, ASBMR 2023. *J Bone Miner Res*. 2024;39(10):1377-1385.

doi: 10.1093/jbmr/zjae110

48. Uenaka M, Yamashita E, Kikuta J, *et al*. Osteoblast-derived vesicles induce a switch from bone-formation to bone-resorption in vivo. *Nat Commun*. 2022;13(1):1066.

doi: 10.1038/s41467-022-28673-2

49. Fischetti T, Borciani G, Avnet S, *et al*. Incorporation/Enrichment of 3D Bioprinted Constructs by Biomimetic Nanoparticles: Tuning Printability and Cell Behavior in Bone Models. *Nanomaterials (Basel)*. 2023;13(14):2040.

doi: 10.3390/nano13142040

50. Zhao Z, Chen X, Chen H, *et al*. Cerium-Containing Mesoporous Bioactive Glass Nanoparticles Reinforced 3D-Printed Bioceramic Scaffolds toward Enhanced Mechanical, Antioxidant, and Osteogenic Activities for Bone Regeneration. *Adv Healthc Mater*. 2025;14(9):e2404346.

doi: 10.1002/adhm.202404346

51. Zhang M, Zhai X, Ma T, *et al*. Sequential Therapy for Bone Regeneration by Cerium Oxide-Reinforced 3D-Printed Bioactive Glass Scaffolds. *ACS Nano*. 2023;17(5):4433-4444.

doi: 10.1021/acsnano.2c09855

52. Li X, Liu B, Pei B, *et al*. Inkjet Bioprinting of Biomaterials. *Chem Rev*. 2020;120(19):10793-10833.

doi: 10.1021/acs.chemrev.0c00008

53. Mota C, Camarero-Espinosa S, Baker MB, Wieringa P, Moroni L. Bioprinting: From Tissue and Organ Development to in Vitro Models. *Chem Rev*. 2020;120(19):10547-10607.

doi: 10.1021/acs.chemrev.9b00789

54. Leucht A, Volz AC, Rogal J, Borchers K, Kluger PJ. Advanced gelatin-based vascularization bioinks for extrusion-based bioprinting of vascularized bone equivalents. *Sci Rep*. 2020;10(1):5330.

doi: 10.1038/s41598-020-62166-w

55. Oh D, Shirzad M, Chang Kim M, Chung E-J, Nam SY.

Rheology-informed hierarchical machine learning model for the prediction of printing resolution in extrusion-based bioprinting. *Int J Bioprinting*. 2023;9(6):1280.

doi: 10.36922/ijb.1280

56. Grijalva Garces D, Strauss S, Gretzinger S, *et al*. On the reproducibility of extrusion-based bioprinting: round robin study on standardization in the field. *Biofabrication*. 2023;16(1):015002.

doi: 10.1088/1758-5090/acfe3b

57. Zhang J, Wehrle E, Adamek P, *et al*. Optimization of mechanical stiffness and cell density of 3D bioprinted cell-laden scaffolds improves extracellular matrix mineralization and cellular organization for bone tissue engineering. *Acta Biomater*. 2020;114:307-322.

doi: 10.1016/j.actbio.2020.07.016

58. Zhang C, Elvitigala KCML, Mubarok W, Okano Y, Sakai S. Machine learning-based prediction and optimisation framework for as-extruded cell viability in extrusion-based 3D bioprinting. *Virtual Phys Prototyp*. 2024;19(1):e2400330.

doi: 10.1080/17452759.2024.2400330

59. Ma W, Lu H, Xiao Y, Wu C. Advancing organoid development with 3D bioprinting. *Organoid Res*. 2025;1(1):25040004.

doi: 10.36922/or025040004

60. Shen M, Wang L, Gao Y, *et al*. 3D bioprinting of in situ vascularized tissue engineered bone for repairing large segmental bone defects. *Mater Today Bio*. 2022;16:100382.

doi: 10.1016/j.mtbio.2022.100382

61. Sun X, Jiao X, Yang X, *et al*. 3D bioprinting of osteon-mimetic scaffolds with hierarchical microchannels for vascularized bone tissue regeneration. *Biofabrication*. 2022;14(3):035008.

doi: 10.1088/1758-5090/ac6700

62. Pitacco P, Sadowska JM, O'Brien FJ, Kelly DJ. 3D bioprinting of cartilaginous templates for large bone defect healing. *Acta Biomater*. 2023;156:61-74.

doi: 10.1016/j.actbio.2022.07.037

63. Wei Q, Peng Y, Chen W, *et al*. Three-dimensional bioprinting for musculoskeletal regeneration and disease modeling. *Int J Bioprinting*. 2024;10(1):1037.

doi: 10.36922/ijb.1037

64. Fan J, Ding Z, Cai Y, *et al*. Revolutionizing Bone Regeneration: Vascularized Bone Tissue Engineering with Advanced 3D Printing Technology. *Aggregate*. 2025;6(4):e731.

doi: 10.1002/agt2.731

65. Shyam Mohan T, Datta P, Nesaei S, Ozbolat V, Ozbolat IT. 3D Coaxial Bioprinting: Process Mechanisms, Bioinks and Applications. *Prog Biomed Eng (Bristol)*. 2022;4(2):022003.

doi: 10.1088/2516-1091/ac631c

66. Shahabipour F, Tavafoghi M, Aninwene GE II, *et al*. Coaxial 3D bioprinting of tri-polymer scaffolds to improve the osteogenic and vasculogenic potential of cells in co-culture models. *J Biomed Mater Res A*. 2022;110(5):1077-1089.

doi: 10.1002/jbm.a.37354

67. Ghahri T, Salehi Z, Aghajanpour S, *et al*. Development of osteon-like scaffold-cell construct by quadruple coaxial extrusion-based 3D bioprinting of nanocomposite hydrogel. *Biomater Adv*. 2023;145:213254.

doi: 10.1016/j.bioadv.2022.213254

68. Zhang J, Suttapreyasri S, Leethanakul C, Samruajbenjakun B. Fabrication of vascularized tissue-engineered bone models using triaxial bioprinting. *J Biomed Mater Res A*. 2024;112(7):1093-1106.

doi: 10.1002/jbm.a.37694

69. Zhou K, Sun Y, Yang J, Mao H, Gu Z. Hydrogels for 3D embedded bioprinting: a focused review on bioinks and support baths. *J Mater Chem B*. 2022;10(12):1897-1907.

doi: 10.1039/d1tb02554f

70. Jalandhra GK, Molley TG, Hung TT, Roohani I, Kilian KA. In situ formation of osteochondral interfaces through "bone-ink" printing in tailored microgel suspensions. *Acta Biomater*. 2023;156:75-87.

doi: 10.1016/j.actbio.2022.08.052

71. Guo C, Wu J, Zeng Y, Li H. Construction of 3D bioprinting of HAP/collagen scaffold in gelation bath for bone tissue engineering. *Regen Biomater*. 2023;10:rbad067.

doi: 10.1093/rb/rbad067

72. Abaci A, Guvendiren M. 3D bioprinting of dense cellular structures within hydrogels with spatially controlled heterogeneity. *Biofabrication*. 2024;16(3):035027.

doi: 10.1088/1758-5090/ad52f1

73. Truong H, Abaci A, Gharacheh H, Guvendiren M. Embedded bioprinting of dense cellular constructs in bone allograft-enhanced hydrogel matrices for bone tissue engineering. *Biomater Sci*. 2025;13(12):3213-3222.

doi: 10.1039/d4bm01616e

74. Zhang H, Luo Y, Hu Z, *et al*. Cation-crosslinked κ-carrageenan sub-microgel medium for high-quality embedded bioprinting. *Biofabrication*. 2024;16(2):025009.

doi: 10.1088/1758-5090/ad1cf3

75. Fang Y, Guo Y, Wu B, *et al*. Expanding Embedded 3D Bioprinting Capability for Engineering Complex Organs with Freeform Vascular Networks. *Adv Mater*. 2023;35(22):e2205082.

doi: 10.1002/adma.202205082

76. Suntornnond R, Ng WL, Huang X, Yeow CHE, Yeong WY. Improving printability of hydrogel-based bio-

inks for thermal inkjet bioprinting applications via saponification and heat treatment processes. *J Mater Chem B*. 2022;10(31):5989-6000.

doi: 10.1039/d2tb00442a

77. Zhu H, Li R, Li S, *et al*. Multi-physical field control piezoelectric inkjet bioprinting for 3D tissue-like structure manufacturing. *Int J Bioprinting*. 2024;10(3):2120.

doi: 10.36922/ijb.2120

78. Gao G, Schilling AF, Yonezawa T, Wang J, Dai G, Cui X. Bioactive nanoparticles stimulate bone tissue formation in bioprinted three-dimensional scaffold and human mesenchymal stem cells. *Biotechnol J*. 2014;9(10):1304-11.

doi: 10.1002/biot.201400305

79. Gao G, Schilling AF, Hubbell K, *et al*. Improved properties of bone and cartilage tissue from 3D inkjet-bioprinted human mesenchymal stem cells by simultaneous deposition and photocrosslinking in PEG-GelMA. *Biotechnol Lett*. 2015;37(11):2349-55.

doi: 10.1007/s10529-015-1921-2

80. Ablanedo Morales P, Rodriguez B, Furth ME, *et al*. Thermal inkjet bioprinting drastically alters cell phenotype. *Biofabrication*. 2023;15(3):031001.

doi: 10.1088/1758-5090/acd3b3

81. Keriquel V, Oliveira H, Remy M, *et al*. In situ printing of mesenchymal stromal cells, by laser-assisted bioprinting, for in vivo bone regeneration applications. *Sci Rep*. 2017;7(1):1778.

doi: 10.1038/s41598-017-01914-x

82. Ng WL, Bartolo P. 3D bioprinting of tissues and organs for systemic diseases and localized injuries. *Mil Med Res*. 2026;13(1):100006.

doi: 10.1016/j.mmr.2026.100006

83. Wang Z, Kumar H, Tian Z, *et al*. Visible Light Photoinitiation of Cell-Adhesive Gelatin Methacryloyl Hydrogels for Stereolithography 3D Bioprinting. *ACS Appl Mater Interfaces*. 2018;10(32):26859-26869.

doi: 10.1021/acsami.8b06607

84. Haghpanah Z, Mondal D, Momenbeitollahi N, *et al*. In vitro evaluation of bone cell response to novel 3D-printable nanocomposite biomaterials for bone reconstruction. *J Biomed Mater Res A*. 2024;112(10):1725-1739.

doi: 10.1002/jbm.a.37719

85. Tao J, Zhu S, Liao X, *et al*. DLP-based bioprinting of void-forming hydrogels for enhanced stem-cell-mediated bone regeneration. *Mater Today Bio*. 2022;17:100487.

doi: 10.1016/j.mtbio.2022.100487

86. Ren X, Wang J, Wu Y, *et al*. One-pot synthesis of hydroxyapatite hybrid bioinks for digital light processing 3D printing in bone regeneration. *J Mater Sci Technol*. 2024;188:84-97.

doi: 10.1016/j.jmst.2024.01.001

87. Hospodiuk M, Dey M, Sosnoski D, Ozbolat IT. The bioink: A comprehensive review on bioprintable materials. *Biotechnol Adv*. 2017;35(2):217-239.

doi: 10.1016/j.biotechadv.2016.12.006

88. Gupta T, Ghosh SB, Bandyopadhyay-Ghosh S, Sain M. Is it possible to 3D bioprint load-bearing bone implants? A critical review. *Biofabrication*. 2023;15(4):042003.

doi: 10.1088/1758-5090/acf6e1

89. Badhe RV, Chatterjee A, Bijukumar D, Mathew MT. Current advancements in bio-ink technology for cartilage and bone tissue engineering. *Bone*. 2023;171:116746.

doi: 10.1016/j.bone.2023.116746

90. Chiticaru EA, Ionita M. Commercially available bioinks and state-of-the-art lab-made formulations for bone tissue engineering: A comprehensive review. *Mater Today Bio*. 2024;29:101341.

doi: 10.1016/j.mtbio.2024.101341

91. Rasouli R, Sweeney C, Frampton JP. Heterogeneous and Composite Bioinks for 3D-Bioprinting of Complex Tissue. *Biomed Mater Devices*. 2025;3(1):108-126.

doi: 10.1007/s44174-024-00171-7

92. Hoppe A, Guldal NS, Boccaccini AR. A review of the biological response to ionic dissolution products from bioactive glasses and glass-ceramics. *Biomaterials*. 2011;32(11):2757-74.

doi: 10.1016/j.biomaterials.2011.01.004

93. Li Z, Xiang S, Lin Z, *et al*. Graphene oxide-functionalized nanocomposites promote osteogenesis of human mesenchymal stem cells via enhancement of BMP-SMAD1/5 signaling pathway. *Biomaterials*. 2021;277:121082.

doi: 10.1016/j.biomaterials.2021.121082

94. Niknam Z, Hosseinzadeh F, Shams F, *et al*. Recent advances and challenges in graphene-based nanocomposite scaffolds for tissue engineering application. *J Biomed Mater Res A*. 2022;110(10):1695-1721.

doi: 10.1002/jbm.a.37417

95. Li C, Sun F, Tian J, *et al*. Continuously released Zn(2+) in 3D-printed PLGA/beta-TCP/Zn scaffolds for bone defect repair by improving osteoinductive and anti-inflammatory properties. *Bioact Mater*. 2023;24:361-375.

doi: 10.1016/j.bioactmat.2022.12.015

96. Nitschke BM, Beltran FO, Hahn MS, Grunlan MA. Trends in bioactivity: inducing and detecting mineralization of regenerative polymeric scaffolds. *J Mater Chem B*. 2024;12(11):2720-2736.

doi: 10.1039/d3tb02674d

97. Wang Z, Sun Y, Li C. Advances in 3D printing technology for preparing bone tissue engineering scaffolds from biodegradable materials. *Front Bioeng Biotechnol*. 2024;12:1483547.

doi: 10.3389/fbioe.2024.1483547

98. Bharadwaj T, Chrungoo S, Verma D. Self-assembled chitosan/gelatin nanofibrous aggregates incorporated thermosensitive nanocomposite bioink for bone tissue engineering. *Carbohydr Polym*. 2024;324:121544.

doi: 10.1016/j.carbpol.2023.121544

99. Zhu Y, Yu X, Liu H, *et al*. Strategies of functionalized GelMA-based bioinks for bone regeneration: Recent advances and future perspectives. *Bioact Mater*. 2024;38:346-373.

doi: 10.1016/j.bioactmat.2024.04.032

100. Korkeamäki JT, Silen R, Syverud K, Mustafa K, Rashad A, Miettinen S. Optimizing gelatin methacryloyl-based bioinks with nanohydroxyapatite for 3D bioprinting in bone tissue engineering. *Bioprinting*. 2026;56:e00479.

doi: 10.1016/j.bprint.2026.e00479

101. Kang Y, Xu J, Meng L, *et al*. 3D bioprinting of dECM/Gel/QCS/nHAp hybrid scaffolds laden with mesenchymal stem cell-derived exosomes to improve angiogenesis and osteogenesis. *Biofabrication*. 2023;15(2):024103.

doi: 10.1088/1758-5090/acb6b8

102. Coşkun S, Akbulut SO, Sarikaya B, Cakmak S, Gumusderelioglu M. Formulation of chitosan and chitosan-nanoHAp bioinks and investigation of printability with optimized bioprinting parameters. *Int J Biol Macromol*. 2022;222(Pt A):1453-1464.

doi: 10.1016/j.ijbiomac.2022.09.078

103. Korkeamäki JT, Rashad A, Ojansivu M, *et al*. Systematic development and bioprinting of novel nanostructured multi-material bioinks for bone tissue engineering. *Biofabrication*. 2025;17(2):025005.

doi: 10.1088/1758-5090/ada63b

104. Allen NB, Abar B, Johnson L, Burbano J, Danilkowicz RM, Adams SB. 3D-bioprinted GelMA-gelatin-hydroxyapatite osteoblast-laden composite hydrogels for bone tissue engineering. *Bioprinting*. 2022;26:e00196.

doi: 10.1016/j.bprint.2022.e00196

105. Bhattacharyya A, Janarthanan G, Kim T, *et al*. Modulation of bioactive calcium phosphate micro/nanoparticle size and shape during in situ synthesis of photo-crosslinkable gelatin methacryloyl based nanocomposite hydrogels for 3D bioprinting and tissue engineering. *Biomater Res*. 2022;26(1):54.

doi: 10.1186/s40824-022-00301-6

106. Indurkar A, Heid S, Bauer J, *et al*. Amorphous calcium phosphate reinforced alginate-dialdehyde-gelatin (ADA-GEL) bioink for biofabrication of bone tissue scaffolds. *Carbohydr Polym Technol Appl*. 2025;9:100710.

doi: 10.1016/j.carpta.2025.100710

107. Wu YF, Wen YT, Salamanca E, *et al*. 3D-bioprinted alginate-based bioink scaffolds with beta-tricalcium phosphate for bone regeneration applications. *J Dent Sci*. 2024;19(2):1116-1125.

doi: 10.1016/j.jds.2023.12.023

108. Bhattacharyya A, Khatun MR, Narmatha S, Nagarajan R, Noh I. Modulation of 3D Bioprintability in Polysaccharide Bioink by Bioglass Nanoparticles and Multiple Metal Ions for Tissue Engineering. *Tissue Eng Regen Med*. 2024;21(2):261-275.

doi: 10.1007/s13770-023-00605-1

109. Sánchez-Rodríguez VH, Pérez-Cortez JE, Gallegos-Martínez S, *et al*. Light-based and cost-effective bioprinting of musculoskeletal GelMA constructs enriched with mesoporous bioactive glass nanoparticles. *Int J Bioprinting*. 2024;10(4):1830.

doi: 10.36922/ijb.1830

110. Kolan KCR, Saxena A, Bromet BA, *et al*. Bioprinting with adipose stem cells and hydrogel modified with bioactive glass. *Int J Bioprinting*. 2024;10(2):2057.

doi: 10.36922/ijb.2057

111. Kiaee G, Dimitrakakis N, Sharifzadeh S, *et al*. Laponite-Based Nanomaterials for Drug Delivery. *Adv Healthc Mater*. 2022;11(7):e2102054.

doi: 10.1002/adhm.202102054

112. Kim J, Choi HS, Kim YM, Song SC. Thermo-Responsive Nanocomposite Bioink with Growth-Factor Holding and its Application to Bone Regeneration. *Small*. 2023;19(9):e2203464.

doi: 10.1002/smll.202203464

113. Chandra DK, Reis RL, Kundu SC, Kumar A, Mahapatra C. Nanomaterials-Based Hybrid Bioink Platforms in Advancing 3D Bioprinting Technologies for Regenerative Medicine. *ACS Biomater Sci Eng*. 2024;10(7):4145-4174.

doi: 10.1021/acsbiomaterials.4c00166

114. Zhang H, Qin C, Zhang M, *et al*. Calcium silicate nanowires-containing multicellular bioinks for 3D bioprinting of neural-bone constructs. *Nano Today*. 2022;46:101584.

doi: 10.1016/j.nantod.2022.101584

115. Li W, Miao W, Liu Y, *et al*. Bioprinted Constructs that Mimic the Ossification Center Microenvironment for Targeted Innervation in Bone Regeneration. *Adv Funct Mater*. 2021;32(9):2109871.

doi: 10.1002/adfm.202109871

116. Yang J, Chen Z, Gao C, *et al*. A mechanical-assisted post-bioprinting strategy for challenging bone defects repair. *Nat Commun*. 2024;15(1):3565.

doi: 10.1038/s41467-024-48023-8

117. Liu C, Ni S, Wu X, *et al*. Strontium-Modified porous attapulgite composite hydrogel scaffold with advanced angiogenic and osteogenic potential for bone defect repair. *Compos Part A-appl S*. 2024;187:108492.

doi: 10.1016/j.compositesa.2024.108492

118. Liu C, Qin W, Wang Y, *et al*. 3D Printed Gelatin/Sodium Alginate Hydrogel Scaffolds Doped with Nano-Attapulgite for Bone Tissue Repair. *Int J Nanomedicine*. 2021;16:8417-8432.

doi: 10.2147/IJN.S339500

119. Zorron M, Cabrera AL, Sharma R, *et al*. Emerging 2D Nanomaterials-Integrated Hydrogels: Advancements in Designing Theragenerative Materials for Bone Regeneration and Disease Therapy. *Adv Sci (Weinh)*. 2024;11(31):e2403204.

doi: 10.1002/advs.202403204

120. Das A, Roy M, Saha M. Recent advances in biomedical applications of carbon and graphene quantum dots: A review. *Biotechnol Bioeng*. 2024;121(5):1469-1485.

doi: 10.1002/bit.28700

121. Dutta SD, Ganguly K, Hexiu J, Randhawa A, Moniruzzaman M, Lim KT. A 3D Bioprinted Nanoengineered Hydrogel with Photoactivated Drug Delivery for Tumor Apoptosis and Simultaneous Bone Regeneration via Macrophage Immunomodulation. *Macromol Biosci*. 2023;23(9):e2300096.

doi: 10.1002/mabi.202300096

122. Jiang Y, Zhou D, Yang B. 3D bioprinted GelMA/GO composite induces osteoblastic differentiation. *J Biomater Appl*. 2022;37(3):527-537.

doi: 10.1177/08853282221098235

123. Bu W, Xu X, Wang Z, *et al*. Ascorbic Acid-PEI Carbon Dots with Osteogenic Effects as miR-2861 Carriers to Effectively Enhance Bone Regeneration. *ACS Appl Mater Interfaces*. 2020;12(45):50287-50302.

doi: 10.1021/acsami.0c15425

124. Geng B, Li P, Fang F, *et al*. Antibacterial and osteogenic carbon quantum dots for regeneration of bone defects infected with multidrug-resistant bacteria. *Carbon*. 2021;184:375-385.

doi: 10.1016/j.carbon.2021.08.040

125. Tang J, Hu J, Bai X, *et al*. Near-Infrared Carbon Dots With Antibacterial and Osteogenic Activities for Sonodynamic Therapy of Infected Bone Defects. *Small*. 2024;20(49):e2404900.

doi: 10.1002/smll.202404900

126. Wang Y, Li J, Li Y, Yang B. Biomimetic bioinks of nanofibrillar polymeric hydrogels for 3D bioprinting. *Nano Today*. 2021;39:101180.

doi: 10.1016/j.nantod.2021.101180

127. Nelson ML, Burgoyne H, Kouchi FR, *et al*. Graphene and Ti(3)C(2)T(x) MXene Nanomaterial-Infused Bioinks for Mechanical and Electrical Improvement of 3D Bioprinted Scaffolds. *ACS Appl Bio Mater*. 2026;9(2):1142-1155.

doi: 10.1021/acsabm.5c02206

128. Liu X, Miller AL II, Park S, *et al*. Two-Dimensional Black Phosphorus and Graphene Oxide Nanosheets Synergistically Enhance Cell Proliferation and Osteogenesis on 3D Printed Scaffolds. *ACS Appl Mater Interfaces*. 2019;11(26):23558-23572.

doi: 10.1021/acsami.9b04121

129. Nie R, Sun Y, Lv H, *et al*. 3D printing of MXene composite hydrogel scaffolds for photothermal antibacterial activity and bone regeneration in infected bone defect models. *Nanoscale*. 2022;14(22):8112-8129.

doi: 10.1039/d2nr02176e

130. Miao Y, Chen Y, Luo J, *et al*. Black phosphorus nanosheets-enabled DNA hydrogel integrating 3D-printed scaffold for promoting vascularized bone regeneration. *Bioact Mater*. 2023;21:97-109.

doi: 10.1016/j.bioactmat.2022.08.005

131. Xu Y, Xu C, He L, *et al*. Stratified-structural hydrogel incorporated with magnesium-ion-modified black phosphorus nanosheets for promoting neuro-vascularized bone regeneration. *Bioact Mater*. 2022;16:271-284.

doi: 10.1016/j.bioactmat.2022.02.024

132. Ojansivu M, Rashad A, Ahlinder A, *et al*. Wood-based nanocellulose and bioactive glass modified gelatin-alginate bioinks for 3D bioprinting of bone cells. *Biofabrication*. 2019;11(3):035010.

doi: 10.1088/1758-5090/ab0692

133. Bedell ML, Torres AL, Hogan KJ, *et al*. Human gelatin-based composite hydrogels for osteochondral tissue engineering and their adaptation into bioinks for extrusion, inkjet, and digital light processing bioprinting. *Biofabrication*. 2022;14(4):045012.

doi: 10.1088/1758-5090/ac8768

134. Li N, Cui J, Chi M, Thieringer FM, Sharma N. Building a better bone: The synergy of 2D nanomaterials and 3D printing for bone tissue engineering. *Materials & Design*. 2023;234:112362.

doi: 10.1016/j.matdes.2023.112362

135. Xu W, Molino BZ, Cheng F, *et al*. On Low-Concentration Inks Formulated by Nanocellulose Assisted with Gelatin Methacrylate (GelMA) for 3D Printing toward

Wound Healing Application. *ACS Appl Mater Interfaces*. 2019;11(9):8838-8848.

doi: 10.1021/acsami.8b21268

136. Dar MA, Xie R, Liu J, *et al*. Current Paradigms and Future Challenges in Harnessing Nanocellulose for Advanced Applications in Tissue Engineering: A Critical State-of-the-Art Review for Biomedicine. *Int J Mol Sci*. 2025;26(4):1449.

doi: 10.3390/ijms26041449

137. Fadeel B, Farcal L, Hardy B, *et al*. Advanced tools for the safety assessment of nanomaterials. *Nat Nanotechnol*. 2018;13(7):537-543.

doi: 10.1038/s41565-018-0185-0

138. Liu JH, Yang ST, Wang H, Chang Y, Cao A, Liu Y. Effect of size and dose on the biodistribution of graphene oxide in mice. *Nanomedicine (Lond)*. 2012;7(12):1801-12.

doi: 10.2217/nnm.12.60

139. Su Z, Chen W, Liang S, *et al*. Multifaceted Characterization for the Hepatic Clearance of Graphene Oxide and Size-Related Hepatic Toxicity. *Molecules*. 2024;29(6):1335.

doi: 10.3390/molecules29061335

140. Ou L, Song B, Liang H, *et al*. Toxicity of graphene-family nanoparticles: a general review of the origins and mechanisms. *Part Fibre Toxicol*. 2016;13(1):57.

doi: 10.1186/s12989-016-0168-y

141. Sui B, Liu X, Sun J. Biodistribution, inter-/intra-cellular localization and respiratory dysfunction induced by Ti(3)C(2) nanosheets: Involvement of surfactant protein down-regulation in alveolar epithelial cells. *J Hazard Mater*. 2021;402:123562.

doi: 10.1016/j.jhazmat.2020.123562

142. Li Y, Jiao H, Zhang H, *et al*. Biosafety consideration of nanocellulose in biomedical applications: A review. *Int J Biol Macromol*. 2024;265(Pt 1):130900.

doi: 10.1016/j.ijbiomac.2024.130900

143. Agarwal T, Onesto V, Banerjee D, *et al*. 3D bioprinting in tissue engineering: current state-of-the-art and challenges towards system standardization and clinical translation. *Biofabrication*. 2025;17(4):042003.

doi: 10.1088/1758-5090/ade47a

144. Perin F, Ouyang L, Lim KS, *et al*. Bioprinted Constructs in the Regulatory Landscape: Current State and Future Perspectives. *Adv Mater*. 2026;38(4):e04037.

doi: 10.1002/adma.202504037

145. Theus AS, Ning L, Jin L, Roeder RK, Zhang J, Serpooshan V. Nanomaterials for bioprinting: functionalization of tissue-specific bioinks. *Essays Biochem*. 2021;65(3):429-439.

doi: 10.1042/EBC20200095

146. Stanco D, Urban P, Tirendi S, Ciardelli G, Barrero J. 3D bioprinting for orthopaedic applications: Current advances, challenges and regulatory considerations. *Bioprinting*. 2020;20:None.

doi: 10.1016/j.bprint.2020.e00103

147. Meng X, Ziadlou R, Grad S, *et al*. Animal Models of Osteochondral Defect for Testing Biomaterials. *Biochem Res Int*. 2020;2020:9659412.

doi: 10.1155/2020/9659412

148. Li Y, Chen SK, Li L, Qin L, Wang XL, Lai YX. Bone defect animal models for testing efficacy of bone substitute biomaterials. *J Orthop Translat*. 2015;3(3):95-104.

doi: 10.1016/j.jot.2015.05.002